

The effect of external tag variation on profile drag of fusiform teleost fish

by

REBECCA SHARON AKHTAR MANOUCHEHRI

B. Sc., Carleton University, 2016

A THESIS SUBMITTED TO THE FACULTY OF GRADUATE
AND POST DOCTORAL AFFAIRS
IN PARTIAL FULFILLMENT OF THE
REQUIREMENTS FOR THE DEGREE OF
MASTER OF SCIENCE

In

Biology

Carleton University

Ottawa, Ontario

© 2018, Rebecca A. Manouchehri

ABSTRACT

The use of external active and passive tags to study locomotion, behaviour, and survival of fish has been common practice for decades. However, if tags significantly impact the organism's routine behaviour, tagging data may not accurately represent the general, untagged population. This study aimed to identify the effects of different external tags on profile drag (as a proxy for cost of transport) of fusiform teleost fish and how different tag attributes (tag size, antenna length, tag shape) affect drag. Chapter 2 used a rigid fish model with an embedded load cell in a water tunnel to compare drag added by tags attached to a fish ("tag drag") across a range of test flow velocities ($0.17\text{-}0.37\text{ m}\cdot\text{s}^{-1}$). Tag drag increased with velocity, but tag shape played a greater role in tag drag magnitude than tag size. Chapter 3 utilized the same apparatus in a factorial study comparing the effect of tag size, shape, and attachment location. The results demonstrated that large, cylindrical tags located anteriorly increase drag more than if they are moved posteriorly, and that small, tapered shaped tags placed at locations other than at the base of the dorsal fin are the least drag-inducing. From these results, it is recommended that tags should be as small as possible and flat; ideally tapered or streamlined rather than protruding and geometric. Tags also should not be placed at the base of the dorsal fin if they are not able to be close to the body wall.

ACKNOWLEDGEMENTS

I would like to thank my co-supervisors, Dr. Steven Cooke and Dr. Jeffery Dawson for their support, expertise, and patience throughout the past two years. Despite some disruptions along the way to the completion of this thesis, their unwavering confidence in my abilities inspired me to persevere. It has been such an incredible learning experience for me, having come from a background somewhat lacking in ecology and conservation, and has given me a new appreciation of fish ecology and fisheries science.

Through the Fish Ecology and Physiology Lab (FECPL) at Carleton, I have had the privilege of meeting and working with some of the most knowledgeable and well-versed in the field of fish ecology. If not for the FECPL, I would never have had opportunities to attend conferences, volunteer for community outreach events, and tag bass for the first time. Thank you all!

From the Department of Biology, I would like to thank Dr. Ryan Chlebak, Sabrina Phoenix, and Mike Jutting for their technical assistance and expertise. I would also like to thank David Raude and Dr. Daniel Feszty and the Department of Mechanical and Aerospace Engineering at Carleton for access to (and use of) their water tunnel.

Of course, none of this would have been possible without the Ottawa-Carleton Institute of Biology and the wonderful folks at the Carleton Graduate Biology office. Thanks for putting up with me when I forgot to book a projector (almost) every time I needed one and for always finding one for me at the last minute!

Finally, thanks to my friends and family, both here in Ottawa and those far away. To my parents, Sharon and Ali, thank you for making learning an integral part of my life and for cultivating an insatiable curiosity in me. To my siblings, Lisa and David, thank you for humouring me and pretending to be as interested in fish biomechanics as I am! And the biggest thanks of all to Matthew: thank you for sticking by my side, supporting me through everything, and believing in me even when I didn't believe in myself.

TABLE OF CONTENTS

ABSTRACT.....	i
ACKNOWLEDGEMENTS.....	ii
TABLE OF CONTENTS.....	iii
LIST OF FIGURES	vi
LIST OF TABLES.....	vii
GLOSSARY	ix
LIST OF ABBREVIATIONS.....	x
STATEMENT OF CONTRIBUTIONS	xi
CHAPTER 1	1
General Introduction.....	1
<i>The “2% rule of thumb”</i>	4
<i>The confounds of behaviour</i>	5
CHAPTER 2	9
Is this tag too draggy? A comparative study of the drag effects of external fish tags on a fusiform teleost fish model.	9
ABSTRACT.....	9
INTRODUCTION.....	11
MATERIALS AND METHODS.....	14
<i>Model creation</i>	14
<i>Model testing</i>	15
<i>Model calibration</i>	17

<i>Data analysis</i>	17
RESULTS.....	19
<i>Model calibration and control data</i>	19
<i>Tag Drag Effects</i>	19
DISCUSSION	21
CHAPTER 3	38
What makes a tag a drag? A comparative study of the drag effects of varying external fish tag size, shape, and attachment locations on a fusiform teleost fish model.....	38
ABSTRACT	38
INTRODUCTION.....	40
METHODS.....	43
<i>Tag creation</i>	43
<i>Experimental data</i>	43
<i>Data analysis</i>	44
RESULTS.....	45
<i>Model calibration and control data</i>	45
<i>Tag drag effects</i>	45
DISCUSSION	47

CHAPTER 4	58
General Discussion	58
LITERATURE CITED	63
APPENDIX.....	69

LIST OF FIGURES

Figure 1.1: Illustration of the drag effects which contribute to profile drag in fish.	8
Figure 2.1: Experimental setup.	28
Figure 2.2: Model with electronic tag attached.	29
Figure 2.3: External tags used for data collection.....	30
Figure 2.4: Calibration apparatus.....	32
Figure 2.5: Profile drag of model (control data).	33
Figure 2.6: Average tag drag of all tags.....	34
Figure 2.7: Tag drag relative to body drag.	35
Figure 2.8: Tag drag at $0.33 \text{ m}\cdot\text{s}^{-1}$	36
Figure 2.9: Effect of antenna on tag drag.	37
Figure 3.1: 3D printed tags and attachment locations.....	53
Figure 3.2: Profile drag of model (control data).	55
Figure 3.3: Average tag drag for all conditions.	56
Figure 3.4: Tag drag at $0.34 \text{ m}\cdot\text{s}^{-1}$	57
Figure A1: Calibration plot for chapter 2 data.....	72
Figure A2: Calibration plot for chapter 3 data.....	74

LIST OF TABLES

Table 2.1: Tag descriptions and dimensions. All measurements were made relative to tag orientation when attached to the fish: x indicates maximum rostrum-caudum measurement (mm), y indicates maximum dorsum-ventrum measurement (mm), z indicates maximum proximal-distal measurement (mm). Note that tags B and F contain two sets of values because of a dual-component design.....	31
Table 3.1: Tag descriptions and dimensions. All measurements were made relative to tag orientation when attached to the fish: x indicates maximum rostrum-caudum measurement (mm), y indicates maximum dorsum-ventrum measurement (mm), z indicates maximum proximal-distal measurement (mm).	54
Table A1: Comparison of trout model measurements and morphological measurements of body parameters collected from museum specimens of lake trout ('lean' variety) as well as the head width-to-total length and peduncle width-to total length ratios.	69
Table A2: Average velocity (V) (m/s), standard error (V SE) (m/s), tag drag (D) (N), and standard tag drag error (F SE) (N) for all tags (A-F) in chapter 2.	72
Table A3: Average water velocity (V) (m/s), standard error of water velocity (V SE) (m/s), average tag drag (D) (N) and standard error of tag drag (D SE) (N) for tag A in chapter 3 at each of the four attachment locations on the fish.....	75
Table A4: Average water velocity (V) (m/s), standard error of water velocity (V SE) (m/s), average tag drag (D) (N) and standard error of tag drag (D SE) (N) for tag B in chapter 3 at each of the four attachment locations on the fish.....	77

Table A5: Average water velocity (V) (m/s), standard error of water velocity (V SE) (m/s), average tag drag (D) (N) and standard error of tag drag (D SE) (N) for tag C in chapter 3 at each of the four attachment locations on the fish..... 79

GLOSSARY

Boundary layer: in fluid dynamics, the thin fluid layer which comes into contact with the surface of a solid body.

Cost of transport: quantifies the energy efficiency of movement by considering the metabolic energy required to move a unit mass of animal a unit distance.

Electronic tag: external telemeter which either transmits acoustic/radio signals via a power source (most often a battery), or archives data internally (in this study, the term is used synonymously with “transmitter”).

Laminar: in fluid dynamics, referring to ordered flow, where fluid layers/sheets flow smoothly together in a unilateral direction.

Profile/Form drag: all resistive forces exerted on a solid object moving through a fluid environment.

Pressure drag: also referred to as form drag, it arises from unequal distribution of pressure along the chord/characteristic length of a solid object, where the pressure is concentrated at the site of initial flow separation. It is a product of cross-sectional area.

Passive tag: any external tag not requiring a built-in power source. Generally used for identification of individuals (often used in combination with an electronic tag).

Skin friction drag/Friction drag: arises from interactions between skin surface and the boundary layer traveling in different directions with different velocities. It is proportional to the wettable area.

Tag: in the context of this paper, refers to any external tag attached to fish, passive or electronic.

Transmitter: external telemeter which transmits acoustic and/or radio signals (in this research, the term is used synonymously with “electronic tag”).

Turbulent: in fluid dynamics, referring to a disordered flow where there is mixing of fluid layers/sheets, leading to changes in fluid velocity and pressure.

Wake: a region of disturbed fluid flow downstream of an object moving with respect to a fluid. Characterized by turbulence and separation of flow. Streamlining often reduces the magnitude of the wake behind an object.

LIST OF ABBREVIATIONS

ABS: acrylonitrile butadiene styrene

COT: cost of transport

STATEMENT OF CONTRIBUTIONS

BA Manouchehri held primary responsibility for designing the research project, collecting and analyzing data, and preparing manuscripts, using established experimental protocols, and a previously-constructed fish model. Writing of all chapters was completed by BA Manouchehri. JW Dawson and SJ Cooke provided comments and feedback on the manuscript. The plastic fish model used was courtesy of Dr. Ryan J. Chlebak (Carleton University).

CHAPTER 1

General Introduction

Affixing tags and devices to animals to track their whereabouts or for individual identification is common practice in wildlife studies. While the practice of tagging or marking animals has been employed by farmers and scientists for decades, the first published study that made use of electronic tagging (radio telemetry) was conducted by LeMunyan and colleagues (1959) (cited in Mech 1983 and Gutema 2015). The development of biotelemetry was revolutionary for the time and has since become a widely used method for data collection in wildlife studies (Cooke et al. 2004).

Over the past six decades, the practice of tagging (and the development of biotelemetry) has substantially changed and has been used to obtain a large volume of data from a wide range of animal taxa, including birds, mammals, and fish (Bannasch 1994; Cooke et al. 2004; Gutema 2015; Mech 1983; Wilson 2011). Tags and electronic transmitters are especially valuable for the study of organisms that do not primarily locomote on land, as they allow for data collection in environments typically inaccessible to researchers. Also, conventional direct human observation (e.g. by divers) may affect behaviour; thus, tags allow for undisturbed observation. In particular, these data have contributed significantly to the disciplines of fisheries sciences and conservation ecology,

having a particularly large impact in the creation and subsequent implementation of conservation efforts (Drenner et al. 2012).

Drag and assumptions of tagging

A key assumption of tagging practice is that the device does not interfere with the animal's natural behaviour, including its locomotion (Drenner et al. 2012; Jacobson and Hansen 2004; Ross and McCormick 1981). Animals that locomote in water challenge the aforementioned assumption due to hydrodynamics (Maddock et al. 1991). All solid objects that locomote in a fluid environment are subject to drag forces resulting from interactions between the body and the fluid, particularly when the fluid is relatively dense (e.g., water) (Webb 1971). This drag force describes the opposing forces that must be overcome for the solid body to achieve forward motion (Vogel 2013; Webb 1975). Due to the high density of water relative to air, hydrodynamic drag forces have a greater impact on swimming movement than drag forces experienced by, for example, a bird flying in air (Webb and Weihs 1983).

An externally affixed tag on a swimming organism will always increase the drag experienced by the organism. However, the drag effect may be small and/or effectively negligible as is often assumed in the practice of tagging. A reduction in drag caused by a tag can be achieved in only three ways – 1) the tag can be made smaller, 2) the tag can be affixed to an organism in a location that minimizes the drag caused by the tag, or 3) the tag can be shaped so as to be less drag inducing (e.g. streamlined) (Thorstad et al. 2013). Additionally, external devices may impede the natural body movements of a fish, thus affecting the biomechanics of propulsion and stability control (Blake 1983; Jepsen et al.

2015). Devices may also interfere with drag reducing mechanisms that act to maintain a laminar boundary layer, such as mucous excretion of the skin (Blake 1983).

Drag forces acting on a fish in forward motion are affected by both the size and shape of the fish and also the undulatory movements of the fish generating thrust and maintaining stability (Shadwick and Lauder 2006; Webb and Weihs 1983). Considering the body alone, the interaction of the surface of the fish with the fluid adjacent to the body (i.e. the boundary layer) produces a “skin friction” (Vogel 2013). This frictional drag component is proportional to the surface area of the fish (i.e. the wettable area) (Blake 1983). Additionally, as the fish moves forward it must physically displace the fluid around its body and so the size of the fish (its volume, dimensions, and shape) results in a greater pressure at the rostral end of the fish relative to the caudal end. This is “pressure drag” and the magnitude depends on the density of water and the velocity of the fish moving through the water. The sum of skin friction drag and pressure drag is termed profile drag and is used to describe all drag forces acting on fish (Figure 1.1) (Webb 1975; Webb and Weihs 1983).

It is necessary to empirically measure profile drag, as mathematical models and computational approaches either can not account for the complexity of form or require specialized computational techniques. These approaches, by definition, only yield predictions of the drag forces acting on a particular body under specified (often constrained) conditions (Blake 1983; Fox et al. 2006; Webb and Weihs, 1983). Even if a numerical model was derived to integrate all the viscous and pressure drag of a complex body shape, it would not be able to account for the orientation effects on boundary layer separation and wake size (Alexander 1990). To date, drag has been measured in studies

through the use of calibrated load cells fixed to a stationary fish (rigid model, anesthetized fish, or preserved specimen) in a water tunnel at varying velocities and it must be noted that these models, anesthetized or preserved specimens will not possess the attributes of a living fish (e.g. movements and surface features/condition) (Blake 1983; Shadwick and Lauder 2006).

The “2% rule of thumb”

Commercially available external tags and data loggers for fish typically range in mass from under 0.25 g to well over 30 g (tag specs from Advanced Telemetry Systems, Inc.). There are no official regulations regarding tag size, shape, weight, or attachment techniques, but common practice is for device weight not to exceed 2% of the weight of the fish (out of water) (Winter 1983; reviewed in Jepsen et al. 2013). However, the rationale for this “2% rule of thumb” has fallen under heavy criticism (see Brown et al. 1999; Jepsen et al. 2005). Published studies have demonstrated that actual tag load varies greatly across species, and that restricting tag size to 2% (or less) of body mass may not ensure that the tag effects are negligible. For example, a study of *Dicentrarchus labrax* (sea bass) found that tags larger than 1% of body mass resulted in a 28% increase in metabolic scope (Lefrançois et al. 2001). Conversely, Brown and colleagues (1999) determined that juvenile *Oncorhynchus mykiss* (rainbow trout) could be implanted with tags up to 12% of their body mass without exhibiting reduced swimming performance.

Although researchers endeavour to place and affix external telemetric devices in a manner they believe does not affect locomotion or the metabolic cost of transport, it is important to quantitatively determine the effects of placement on the body (Jepsen et al., 2015; Kölzsch et al., 2016; Frost et al., 2010). In order to maintain maximal data

relevance, researchers that utilize external tags and data loggers should measure the effect of tracking device presence on profile drag of the species being studied.

The confounds of behaviour

In the literature, studies attempting to classify/identify drag effects often produce contradictory results (Drenner et al. 2012; Jepsen et al. 2005). This is a product of individual variability, and any study using live specimens will be subject to its confounds (Broell et al. 2016). In addition, it is impossible to separate behavioural effects from any physiological effects when studying live organisms. The invariable link between physiology and behaviour means that the only way to obtain data on biomechanical effects, free from the confounds of behaviour, is to use non-living models as proxies. This method has been used infrequently in biomechanics to distinguish actual drag effects due to the criticisms that arise from using a rigid model to approximate a living organism (Webb 1971 and 1975).

Traditionally, the actual drag values obtained from “dead drag” (towing dead or frozen animals through a water tank) or using a rigid, wooden model in a wind tunnel were orders of magnitude different from actual drag values experienced by living organisms. Currently, improvements in technology (3D computer modeling, scanning, and printing) have presented a much more elegant solution for measuring drag without behavioural confounds. With the ability to create highly accurate models, designed from measurements taken of live fish or preserved specimens, it is expected that measured drag would more closely approximate that of a live fish. However, regardless of the drag values themselves, the value of using rigid models is to determine relative tag drag effects in a highly controlled, very repeatable manner. These results provide a starting

point for researchers to design studies using live specimens, focusing on verifying the relevant/significant results.

Thesis objectives and rationale

The vast majority of fish targeted for telemetric studies are from the family Salmonidae and the subfamily Salmoninae (salmon, trout, and char) (Hubbs and Lagler, 2004). This is largely due to the fact that these fish historically have been a very important part of the economy for many communities in the Great Lakes region (Drenner et al., 2012). Various telemetry and tagging techniques have been – and continue to be – used to try and pinpoint causes of population decline and to follow-up on conservation plans and their effectiveness (Cooke et al. 2004; Drenner et al. 2012).

Despite the fairly extensive use of tagging, the majority of studies (66.2%) fail to assess or acknowledge potential tagging/handling effects (Drenner et al. 2012). This highlights a need for evaluation and assessment of tag effects in order to determine the validity of the data presented in these studies. Ideally, both tagging and handling effects can be studied in isolation (given the inseparable link between behaviour and physiology) to determine best practices for tag attachment and tag design.

The objectives of this thesis are to identify tag drag effects of existing external tags commonly used in the field, and to characterize effects specific to varying tag attributes (size, shape, attachment location). Using a rigid fish model mounted on a sting with a load cell and immersed in a water tunnel, drag measurements will be taken for the model alone to determine a baseline drag. The drag will be measured for these at stepped increases in a range of biologically-relevant water velocities ($0.17\text{-}0.37\text{ m}\cdot\text{s}^{-1}$) for cruising lake trout in slow-moving flows. Excising out tag effects will require subtracting

the control data (the model alone) from the total measured drag (model with tag attached). This “tag drag” will allow for more direct comparison between actual tag effects in order to determine which tag attributes have the largest effect on drag. Chapter 2 will focus on the tag drag effects of six existing external tags attached at the lateral musculature proximal to the dorsal fin. Chapter 3 will investigate the effects of attachment location, tag size, and tag shape using 3D printed tags of three different shapes and three sizes. All tags will be tested at all attachment locations and the results analyzed to determine the attributes which may be the most drag inducing.

The results of these studies will be used to suggest guidelines for tag design/attachment parameters on fusiform teleost fish in Chapter 4. To the author’s knowledge, this is the first such study to be conducted using a 3D printed model and 3D printed tags to systematically determine drag effects of different tag attributes and attachment locations. It is expected that the results of this study may be used to design and implement experiments using live specimens to verify the tag drag effects, to inform common practice, and potentially to create a set of guidelines for tag designs and attachment locations ideal for fusiform teleost fish.

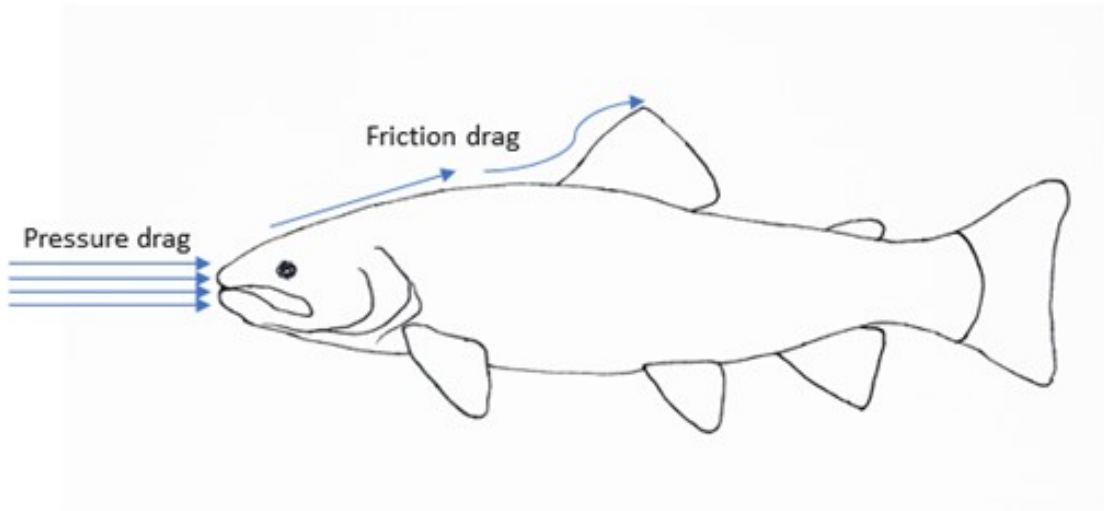


Figure 1.1: Illustration of the drag effects which contribute to profile drag in fish.

CHAPTER 2

Is this tag too draggy? A comparative study of the drag effects of external fish tags on a fusiform teleost fish model.

ABSTRACT

External markers and electronic tags are commonly employed by fisheries scientists to study the ecology of fish. The validity of the data collected from tagging relies on the assumption that the tag does not significantly impact behaviour, condition, or survival. This study focused on drag effects (as a proxy for cost of transport (COT)) of different external tags without the confounds of behaviour through use of a static (plastic) model in a water tunnel. Drag was measured with calibrated load cells fixed to a 3D-printed *Salvelinus namaycush* rigid model in a water tunnel. Six external tags of different dimensions (of appropriate scale for the model size) were individually affixed to the model at the same site and total body drag (profile drag) was measured over stepped increases in water velocity ($0.17 \text{ m}\cdot\text{s}^{-1}$ to $0.37 \text{ m}\cdot\text{s}^{-1}$). Tag attachment resulted in an increase in profile drag with increased water velocity. Most tags reached a maximum force magnitude at an average velocity of $0.33 \text{ m}\cdot\text{s}^{-1}$. When drag due to the tag was calculated as percent of total body drag, values were highest at low velocities and lower at higher velocities. Most tags showed a peak in drag at water velocities approximating

0.20 m•s⁻¹. Tags with the greatest depth (e.g., cylindrical electronic tags) produced more drag at all water velocities than more streamlined tags (e.g., anchor tags). The results of this study suggest that tag shape inherently has more influence on COT than tag size, as increased drag is usually accompanied by a higher COT. This has implications for species-specific tag design and highlights the need for more studies examining hydrodynamic tag effects on fish.

INTRODUCTION

The practice of tagging fish for research and differentiation between individuals has been used for centuries (Thorsteinsson 2002). Although some tag types can be inserted into the body cavity or tissue such that there is nothing external to the fish's body (e.g. intracoelomic, gastric, oviduct, subdermal or intramuscular insertion; reviewed in Bridger and Booth 2003 and Cooke et al. 2012), there are still many tag types and/or reasons that lead to tags being placed externally (Jadot 2003; Johnson et al. 2015). Fish tags can be broadly divided into two categories: active tags, which require a power source, and passive tags, which are used for individual identification (Drenner et al. 2012). Passive tags have been used by fisheries professionals, researchers, and even fishers for decades (since mid-1900s if not earlier; reviewed in Jones 1979; Nielsen 1992; Parker et al. 1990) for their low cost of production and relatively easy attachment process with low tagging-associated mortality (Thorsteinsson 2002). Active (radio/acoustic) tags or biologging devices provide researchers with the potential to collect an assortment of detailed data (e.g. locational, physiological, and environmental; reviewed in Cooke et al. 2012; Lucas and Baras 2000) but are comparatively larger due to the need for an internal power source. Recent innovations have allowed for the creation of smaller active tags, making it vital that the effects of varying tag shapes and sizes are identified for various species in order to design tags that will cause the smallest load increase possible.

Although tagging is one of the most widely-used data collection techniques in fish and wildlife studies, it remains a controversial practice due to the potential impact of tagging on individual animal condition, behaviour and survival – their welfare (Bridger and Booth 2003; Cooke et al. 2013; Gutema 2015; Ross and McCormick 1981; Wilson

2011). Part of the debate stems from the complexity of tag effects, causing inconsistent and contradictory results amongst studies (Wilson 2011; Wilson et al. 2015). One way in which researchers attempt to separate biomechanical effects from behavioural effects is through the use of models in wind and water tunnels to isolate drag effects of external tags (Arnold and Holford 1978; Harris 1938; Jones et al. 2011; Vandenabeele et al. 2015). Drag refers to the opposing forces experienced by an object moving through a fluid as a product of hydro/aerodynamics and is often used to estimate changes in cost of transport (Jones et al. 2011). To date, most studies involving tagging effects on fish focus on aspects of tag retention, behaviour, condition (e.g., growth rate), swimming ability or survival with few attempts to take a more mechanistic approach to identify if and how external tags – especially aspects of their size or shape – influence drag.

The objective of this paper was to identify the effect of commonly employed external tags on profile drag using a prototypical teleost fish with fusiform body shape – the lake trout (*Salvelinus namaycush*). Because drag scales to the second power of swimming (or water) velocity, and in proportion to object size, it was hypothesized that a tag at higher water velocity would produce more drag than at lower water velocity, and that larger tags would produce more drag than smaller tags. However, it is well-known that for complex (non-geometric) shapes, drag must be determined empirically because of the complex interactions of surface area, placement relative to other (body) structures, and flow characteristics (Fox et al. 2006). In this study, comparisons were made between six external tags selected to represent a variety of passive and active (telemetry) configurations typical of common practice (Figure 2.2, Table 2.1). A dart tag and Petersen disc tag were selected to represent some of the most popular passive external

fish tags. Four electronic tags of comparable sizes but different shapes and dimensions were selected to represent commonly-used active tags (Figure 2.3, Table 2.1). Tags were specifically selected to demonstrate drag effects of diverse shapes and dimensions, including varying antenna length, and lack of antenna on radio tags. The results of this experiment are intended to inform research, identifying potential aspects of tag design which may have a greater or lesser impact on drag effects, and providing a basis for future studies using live specimens.

MATERIALS AND METHODS

Drag effects were determined by affixing existing external tags to a 3D printed lake trout model in a water tunnel. The model was mounted on a sting containing a custom-built load cell oriented to measure profile (whole body) drag (Figure 2.1). Water velocity was increased by steps and the profile drag forces measured for each tag over a range of biologically relevant water velocities for cruising lake trout in slow-moving water flows.

Model creation

A biologically accurate, appropriately scaled, physical model of a lake trout was used for data collection. Morphological measurements from preserved trout specimens ('lean' variety) were collected at the Canadian Museum of Nature (Research labs and collections facility – located in Gatineau Quebec). Specimens, preserved in alcohol, were photographed (Nikon D60 on a copy stand with suitable lighting and scale reference) with care taken to avoid perspective distortion. Measurements were made directly using calipers and from digital images using ImageJ software. Key landmark locations for measurements included the snout to tail fork, and dorsum to ventrum and body thickness viewed from the dorsum (Table A1 in appendix). These measurements and photographs, combined with values found in literature (Muir et al. 2014), were then used to create a digital 3D model using 3D Studio Max software (v. 8.0, San Rafael, CA). This process involved using an imported image of a lake trout, viewed from the side, where a digital 'wire mesh' was then traced/created from the imported image. This procedure allowed for the creation of an arbitrary number of vertices that allowed the morphologically

measured landmarks (operculum, eyes, fins, mouth, etc.) to be accurately positioned on the digital rendering.

Once complete, a stereolithography file (.STL) was produced from the digital rendering. The model was isometrically scaled and printed in acrylonitrile butadiene styrene (ABS) plastic using a 3D printer (rapid-prototyper) (MakerBot Replicator 2X) that had been customized and optimized for printing ABS plastic in high resolution. The model was printed in sections to accommodate the print capacity of the printer (build plate measured 15 cm by 25 cm and was limited to 12 cm tall objects) then assembled using marine grade silicone adhesive. The model was validated by comparing measurements from the model with those obtained from the literature actual specimens (Table A1).

Load cells (5 kg) were purchased commercially (RobotShop.com) and installed where the sting attached to the model (Figure 2.1). Signals from the load cells were amplified with a custom-built strain gauge amplifier and captured using a digital multimeter with sample and hold functions. This amplifier produced linear output over the range of forces expected in the tests that were performed (see calibration procedure below). For each experiment, the model (40 cm total length) was suspended to measure axial loads. As confirmed by testing prior to experimental data collection, the model was insensitive to lateral (yaw) and dorsal-ventral (pitch) applied forces.

Model testing

Tests were completed in a Rolling Hills Research Corporation (model 2436) water tunnel located at Carleton University in the Department of Mechanical and Aerospace Engineering. This water tunnel has a test section measuring 0.6 m wide x 0.9

m deep with a length of 1.8 m. With no model in the test section, flow was laminar from velocities of $0.17 \text{ m}\cdot\text{s}^{-1}$ to $0.37 \text{ m}\cdot\text{s}^{-1}$ (turbulence intensity $< 1.0\%$ RMS; velocity uniformity $< \pm 2\%$; mean flow angularity $< \pm 1.0^\circ$ in pitch and yaw). Maximum water velocity used for testing was restricted by the maximum flow which could be produced by the water tunnel ($0.37 \text{ m}\cdot\text{s}^{-1}$).

For testing, the model was attached to a rigid aluminum sting with a streamlined cowling within the test section of the water tunnel. The model was centered to minimize edge effects from the water tunnel walls. In preliminary tests (Calculation A1 in appendix), blockage corrections were less than 4% and therefore were not applied to the reported water velocity. Total drag force (in Newtons) was measured for stepped increases in water velocity from $0.17 \text{ m}\cdot\text{s}^{-1}$ to $0.37 \text{ m}\cdot\text{s}^{-1}$; at each step, the water tunnel was allowed to stabilize to a consistent velocity of flow before measurements were taken.

Six external tags were selected for the study with dimensions and characteristics reported in Table 2.1 and Figure 2.3. These tags were affixed to the area corresponding with dorsal fin musculature on the left side of the model (15cm from snout) with hot glue (Stanley® DualMelt hot-glue, model STHT1-70430) (Figure 2.2). The hot-glue attachment method was assumed to not contribute to the measured drag forces (i.e. the tags on the model fish in this study are assumed to be hydrodynamically similar to the same tags attached to a live fish). Moreover, the tags were positioned in a way to emulate how they appear when attached to a live fish (e.g., the radio tag antenna is not secured, the anchor tag is only secured at the proximal anchor end). All tags followed the “2% rule-of-thumb,” a tagging guideline which suggests tag mass should be less than 2% of the fish’s body mass to prevent significant impact on swimming ability (Winter 1983;

Winter 1996; reviewed in Brown et al. 1999 and Jepsen et al. 2005), using an estimate of fish weight based on body length, thus representing acceptable tag sizes used for mature *S. namaycush* in the field (Muir et al. 2014).

Each of the external tags (Figure 2.3, Table 2.1) were attached individually and total body drag measured from $0.17 \text{ m}\cdot\text{s}^{-1}$ to $0.37 \text{ m}\cdot\text{s}^{-1}$. Control data collection (profile drag values for $0.17 \text{ m}\cdot\text{s}^{-1}$ to $0.37 \text{ m}\cdot\text{s}^{-1}$ water velocity) was repeated four times in total and each experimental test repeated twice. Note that tag D strain gauge readings were taken at slightly different velocities than the other tags due to a switch in personnel operating the water tunnel velocity controls.

Model calibration

For calibration, the model was suspended in a specially designed apparatus (Figure 2.4) that mimicked the position of the fish in the flow of water in the water tunnel. A string and pulley system with known weights was used to apply axial loads (along the body length of the model) to simulate different drag loads. Because the weights were suspended under the influence of gravity, drag force was determined as mass multiplied by acceleration due to gravity ($9.80632 \text{ m}\cdot\text{s}^{-2}$) (Preston-Thomas et al. 1960). A plot of force (in N) and instrument reading (in mV) verified the linear relationship between the two variables over the entire range of expected drag forces from the model in the water tunnel (Figure A1 in appendix).

Data analysis

Control data were used to calculate profile drag (N) of the model on the sting and determine the relationship between water velocity ($\text{m}\cdot\text{s}^{-1}$) and profile drag (N). In order to isolate tag effects, control mean profile drag was subtracted from the mean total body

drag values measured for each tag. Percent contribution of the tag to overall profile drag was also calculated. Given that the relative experimental profile drag values were the primary focus of this research, data has been presented in figures highlighting comparative tag effects in order to convey observed trends. Statistics have not been used to analyze the data because multivariate analysis would reduce the confidence of the results given the sample sizes used in this study. However, standard errors for both variables (water velocity and tag drag) have been calculated and are presented in table format in the appendix (Table A2). Graphs were rendered, and tables created in Microsoft Excel 2016®.

RESULTS

Model calibration and control data

Measured profile drag force increased as water velocity increased (Figure 2.5). Repeated measurements from the model showed the variation in drag between runs was, on average, 15% (SD = 0.008 N). The minimum drag force detectable by the load cell was 0.010 N (dashed line in Figure 2.5) which was obtained at a water velocity of approximately $0.17 \pm 0.003 \text{ m}\cdot\text{s}^{-1}$.

Tag Drag Effects

Tag drag increased for velocities ranging from $0.17 \text{ m}\cdot\text{s}^{-1}$ to $0.37 \text{ m}\cdot\text{s}^{-1}$ (Figure 2.6). The maximum magnitude of the increase ranged from 0.0123 N (tag A, $0.32 \text{ m}\cdot\text{s}^{-1}$) to 0.0189 N (tag C, $0.32 \text{ m}\cdot\text{s}^{-1}$) (Figure 2.6).

When the drag of the tag, expressed as a proportion (%) of body drag (measured without a tag), was calculated for each tag, values tended to be higher at lower velocities (Figure 2.7). Additionally, with the exception of tags A and E, all tags reached a maximum drag effect at water velocities approximating $0.20 \text{ m}\cdot\text{s}^{-1}$ (Figure 2.7): tag C (36.49%); tag D (35.62%); tag B (32.96%), tag F (27.69%) (Figure 2.7). Tags A and E contributed less by percentage to total body drag at 14.55% and 14.55%, respectively (Figure 2.7).

In order to directly compare tag effects, a biologically relevant water velocity of $\sim 0.33 \text{ m}\cdot\text{s}^{-1}$ – the estimated sustained swimming speed for lake trout of comparable size to the model in a relatively ordered flow – was chosen (Dunlop et al. 2010; Stewart et al. 1983) (Figure 2.8). Tag C resulted in the highest average tag drag effects at $0.33 \pm 0.005 \text{ m}\cdot\text{s}^{-1}$ (0.0189 N, SD = 0.0015 N), followed by tags F (0.0158 N, SD = 0.0010 N), D

(0.0133 N, SD = 0.0074), and B (0.0130 N, SD = 0.0000 N). Tags E and A produced slightly smaller drag effects on average (Tag E: 0.0126 N, SD = 0.0005 N; Tag A: 0.00123 N, SD = 0.0000) (Figure 2.8).

DISCUSSION

Although attaching external electronic devices and passive tags to fish is a procedure commonly employed in scientific research, there is a limited understanding of how various aspects of tag design (i.e., shape, relative size) affect fish locomotion. To obtain a clear picture of the precise effect of external tags, in this study, drag produced by tagging a model fish with commonly employed tags was directly measured. It is often assumed that the smaller the device, the less the impact. However, since tags are complex geometric shapes, just as the fish itself is a complex (albeit streamlined) geometric shape, empirical measurements are the only way to determine, with certainty, the effect of a device on drag experienced by a fish (Alexander 1990; Fox et al. 2006; Dunlop et al. 2010).

The objective of this paper was to determine the effect of external tags on profile drag (as a proxy for COT) of a lake trout. Using a rigid model in a water tunnel (velocities ranging from $0.17 \text{ m}\cdot\text{s}^{-1}$ to $0.37 \text{ m}\cdot\text{s}^{-1}$), drag of the model was measured at stepped velocity increases (Figure 2.5). Maximum drag values of 0.120 N at $0.36 \text{ m}\cdot\text{s}^{-1}$, obtained for the 40 cm model alone in this study, are not dissimilar to drag values 0.080 N at $0.38 \text{ m}\cdot\text{s}^{-1}$ of a 30 cm trout model (with a small load attached) as determined by Webb (1971). Likewise, tag drag for a dangling acoustic tag in a water tunnel has been experimentally measured as approximately 0.006 N at a water velocity of $0.32 \text{ m}\cdot\text{s}^{-1}$ (Arnold and Holford 1978), which is comparable to the tag drag of 0.008 N at $0.32 \text{ m}\cdot\text{s}^{-1}$ (tag D, first experimental run) gleaned from this study. The most probable cause for the slight discrepancy between the drag measured in this study and early drag measurements is a product of the rise in 3D printing technology (e.g., computer modeling). Whilst the

measurement profile drag using dead drag (towing a dead or frozen fish through a water tunnel) was revolutionary at the time of its conception, more recent technology (3D printing and computer modelling) has allowed researchers to measure drag in a more sophisticated manner, designed to be more representative of actual profile drag experienced by fish.

As hypothesized, the presence of an external tag increased profile drag of the model, yielding higher drag values at higher water velocities (Figure 2.6). All tags reached a peak drag force at a velocity of $0.33 \pm 0.003 \text{ m}\cdot\text{s}^{-1}$ (in water velocities ranging from $0.17 \text{ m}\cdot\text{s}^{-1}$ to $0.37 \text{ m}\cdot\text{s}^{-1}$) (Figure 2.6). At velocities higher than $0.33 \text{ m}\cdot\text{s}^{-1}$, there was a reduction in drag effects likely due to a change in the flow regime (Figure 2.6). Experimental results indicate that there may have been a flow transition at a velocity of $0.35 \text{ m}\cdot\text{s}^{-1}$ in the water tunnel, given the sudden increase in tag drag (contrary to overall population trend). If this is the case, and the reduction in drag effects is due to an earlier boundary layer separation and a more turbulent wake, it follows that a tag located on the musculature of the dorsal fin may not produce as much drag as in more laminar flows (for a more detailed explanation, see Webb 1975).

It was also observed that a small range of test velocities produced an increase in turbulence in the working section of the water tunnel. This could be due to the mechanical interaction between model, water flow velocity, and test section dimensions. This “resonance” occurred consistently at a velocity of $\sim 0.22 \text{ m}\cdot\text{s}^{-1}$ and resulted in lower than expected measured forces (Figures 2.6-2.7) (see Vickery and Watkins 1964 and Webb 1975 for a more in-depth explanation).

Drag effects were compared through the calculation of percent contribution of the tag to total body drag as a proxy for tag effects on COT (see Fish (1992) for a mathematical model which used dead drag measurements and water velocity to determine thrust and power needed for steady swimming in order to report an estimated COT). In contrast with the drag value trends described previously, tag percent contribution values were higher at lower velocities (Figure 2.7). At water velocities approximating $0.20 \text{ m}\cdot\text{s}^{-1}$, nearly all tags reached a maximum percent contribution well above 20% (Figure 2.7), unlike an early study conducted by Arnold and Holford in 1978, which estimated tag effects of less than 7% on drag and swimming speed of plaice (*Pleuronectes platessa*) and northern cod. However, the Arnold and Holford study used tag drag values obtained by affixing an acoustic tag to a sting and immersing it in a water tunnel in theoretical equations of swimming speed, acceleration, and power to estimate tag effects. As already established in this paper, drag measurements of complex shapes cannot be accurately predicted, but must be measured empirically.

The tag that contributed most to model drag was tag C (36.49%), followed by tag D (35.62%), tag B (32.96%), and tag F (27.69%) (Figure 2.7). The two tags that did not reach maximum percent drag contribution at $\sim 0.20 \text{ m}\cdot\text{s}^{-1}$ were tags A (14.55%) and E (14.55%) (Figure 2.7). This gives rise to a potential underlying mechanism: that profile drag becomes dominated by the effects of the fish body shape as velocity increases, decreasing the contribution of the tag to total body drag. Thus, these data suggest that the energetic cost of a tag will tend to be higher at lower swimming velocities – in the case of tags C, D, and B, over 30% of profile drag was caused by the attachment of tags to the model – but will decrease as velocity increases (Figure 2.7).

In a study conducted by Dunlop and colleagues (2010), integrated multibeam acoustics and biotelemetry were used to quantify *in situ* swimming behaviour of lake trout. They implanted fish with ultrasonic tags and observed their vertical and horizontal movements using hydroacoustics (Dunlop et al. 2010). Their results indicated that, when both vertical and horizontal swimming speeds are taken into account, mean swimming speeds for tagged trout (mean total length = 58.1 ± 11.3 cm) ranged from $0.33 \text{ m}\cdot\text{s}^{-1}$ to $0.77 \text{ m}\cdot\text{s}^{-1}$ (Dunlop et al. 2010). Using the findings of that paper, it was estimated that a 40 cm trout model would likely exhibit mean swimming speeds of $0.33 \text{ m}\cdot\text{s}^{-1} \pm 0.005 \text{ m}\cdot\text{s}^{-1}$. The tag that increased drag the most (and by extension, caused the highest burden) was not the tag with the highest surface area (tag F), but tag C (0.0189 N , $\text{SD} = 0.0025 \text{ N}$) (Figure 2.8). The tag with the highest surface area, tag F, yielded the second largest increase in drag force (0.0158 N , $\text{SD} = 0.0010 \text{ N}$) (Figure 2.8). Both tags have flat surfaces and tall sides (Figure 2.3), which likely caused a disruption in the boundary layer, increasing drag. Tag D (0.0133 N , $\text{SD} = 0.0074 \text{ N}$) has shorter sides and curved edges, which allowed the tag to be more streamlined and decrease drag (burden) (Figure 2.8). Tags, B (0.0130 N , $\text{SD} = 0.0000$), E (0.0126 N , $\text{SD} = 0.0005 \text{ N}$), and A (0.0123 N , $\text{SD} = 0.0000$), all produced smaller drag values than the other tags (Figure 2.8). Tag E has a larger surface area and depth than both A and B, yet tag B yielded a higher drag effect than tag E, demonstrating that tag shape, dimensions, and size alone cannot predict drag effects. This highlights the importance of taking into consideration the swimming speed of the fish to be tagged, as well as the flow regimes when selecting an appropriate external tag.

These results show that the drag experienced by a fish is not easily predicted based on size or shape. Tags with the largest surface area did not produce greater drag forces than all smaller tags. When considering tag effects, tag shape (e.g., smooth, curved shapes versus irregular shapes with straight edges), tag dimensions (e.g., flat and streamlined or deeper and extending further from the body), surface area, and antenna all interact in complex ways at different water velocities and flow regimes (Broell et al 2016).

One aspect of active tag design that is widely debated is the effect of an antenna on tagged individuals. A study conducted by Murchie and colleagues (2004) looked at the effect of antennae on juvenile rainbow trout (*Oncorhynchus mykiss*) implanted with small radio tags attached to dangling antenna. Their results showed that antenna lengths ranging from 15-30 cm impaired swimming ability (regression analysis results: $R^2 = 0.11$, $P < 0.001$) (Murchie et al. 2004). However, these trout were juvenile (mean fork length = 14.8 cm) and the antenna added upwards of 1-2 body-lengths to the fish. In this paper, tags D-F had antenna lengths less than 75% of model total length (Table 2.1), and the tag with the highest drag (tag C) and contribution to overall profile drag did not have an antenna (Figures 2.6-2.8). Tags C and D were of comparable size and surface area with the main difference being the presence of an antenna on tag D. According to the data, the effect of antenna is either too small to be detected with the equipment used in this study or is negligible (Figure 2.9). In fact, at velocities over $0.30 \text{ m}\cdot\text{s}^{-1}$, the tag with antenna produced lower drag values than the tag without an antenna (Figure 2.9).

Qualitative observation of the behaviour of the antenna revealed that, at lower water velocities, the antenna bowed towards the bottom of the tank, but gradually

straightened to become parallel with the model at higher velocities. It is important to consider these results apply to fairly rigid antennae that are shorter than the body length of the tagged fish in a range of test velocities ($0.17 \text{ m}\cdot\text{s}^{-1}$ to $0.37 \text{ m}\cdot\text{s}^{-1}$) and only describe the drag effects of an antenna (i.e. other antenna effects such as fouling, or tangling have not been considered).

The use of a static model has several advantages and disadvantages. Rigid models are unable to produce the undulating movements that result in increased velocity in the boundary layer (and thus an increase of drag), or the external mucous coat that serves to decrease friction (and thus decrease drag) (Alexander 1990; Barrett et al. 1999; Blake 1983). However, the value of using a rigid model is to obtain comparative results relative to a baseline, indicating the overall effect of a transmitter on drag (Arnold and Holford 1978; Webb 1975). The use of a model also allows for an unlimited number of test repetitions, impossible to match in a study using live or preserved specimens. Additionally, if real fish were used, the presence of a transmitter may affect behaviour and, by extension, the biomechanics of swimming, making it difficult to determine the precise effect of a transmitter on profile drag.

As alluded above, the experimental setup provides a high degree of control over confounding variables, producing low variability and high repeatability (Figure 2.5). Variability of water velocity was quite low, with standard deviation never surpassing 1.6% ($\text{SD} = 0.002 \text{ m}\cdot\text{s}^{-1}$) of total velocity at any given point (Figure 2.5). Though there was slightly more variability in the drag force values ($\text{SD} = 0.008 \text{ N}$), the majority of measurements deviated less than 16.2% from the mean (Figure 2.5). In studies with live fish, it is nearly impossible to obtain these low levels of deviation across samples due to

individual variation (e.g., size, state of health, behaviour) (discussed in Jepsen et al. 2015). Thus, the use of a model provides results that more clearly show biomechanical trends without the confounds of individual variation and behaviour.

The results of this study highlight which aspects of tag design may be the most drag-dependent for lake trout or similar teleost fusiform fish in a specific flow regime. These results are intended to be used as a starting point for further studies (see Chapter 3) using live specimens. Future studies should also investigate the role of tag placement and surgical attachment technique on COT and survival of tagged individuals. Dye flow visualization or particle image velocimetry would confirm drag effects attributed to disturbance in flow and streamlining of the model. However, it is important to note that tag effects will differ based on species morphology, swimming mode, and habitat, necessitating species-specific studies (Jepsen et al. 2005; Jepsen et al. 2015; Thorsteinsson 2002).

The presence of an external tag may impact profile drag, and could cause increases in energetic costs, decreasing organism survival and (in the case of a telemetric device), yielding invalid data. There is a major lack of data describing the effect of tags on fish and the extent to which these effects influence the data collected from tagging studies. This highlights the importance of understanding the species-specific effect of tagging on swimming and COT and the need for more studies investigating tag effects. Research of the effect of tags on behaviour, physiology, morphology (in the case of juvenile tagging), and mobility/energetics will provide the data necessary to design species-specific tags and attachment methods/locations which will help minimize tag effects.

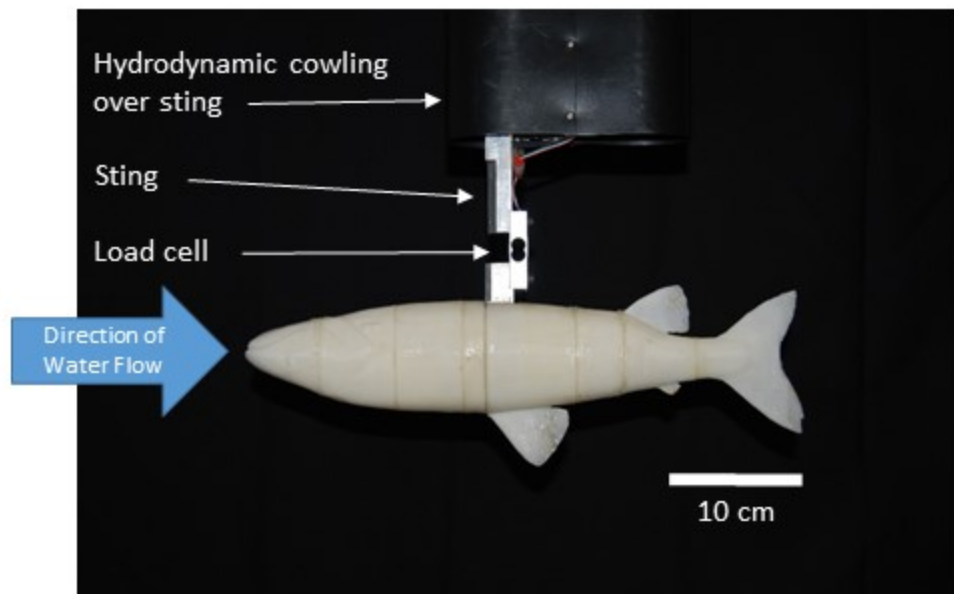


Figure 2.1: Experimental setup. A 40 cm *S. namaycush* model suspended from a sting in a water tunnel. The model was mounted upside-down in the working section of the water tunnel for testing.



Figure 2.2: Photograph of the model with an attached electronic tag to illustrate placement and method of attachment. Inset is an enlarged view of the tag at the base of the dorsal fin.

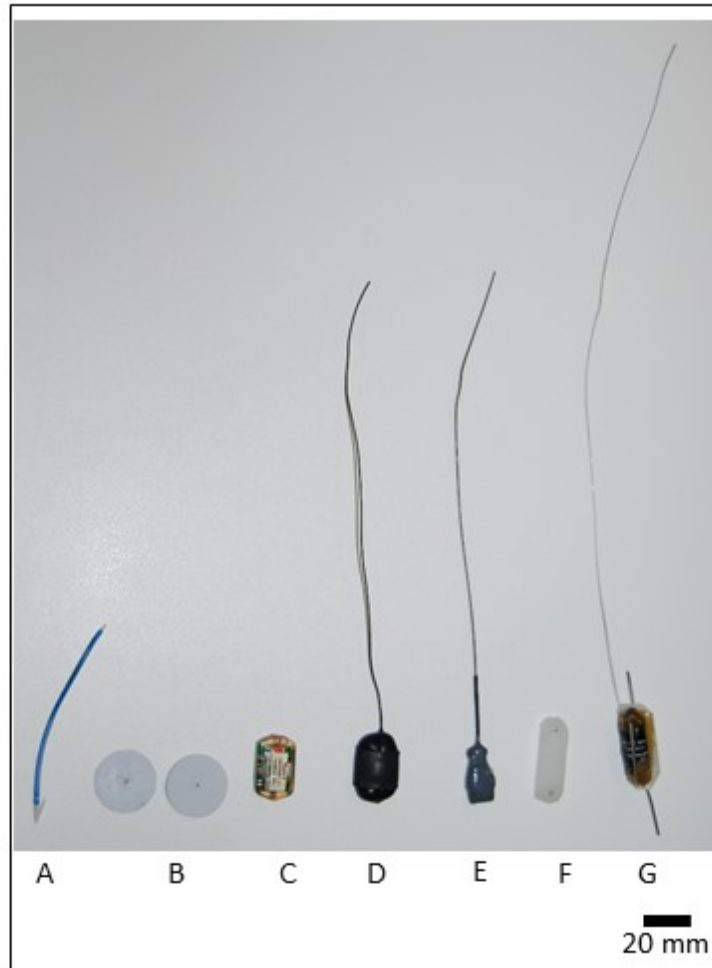


Figure 2.3: Passive and active external tags used for data collection. From left to right: A - dart tag, B - Petersen disc, C - hexagonal archival logger, D - laterally compressed radio tag, E - laterally compressed radio tag, F - applied backing plate and cylindrical radio tag (G).

Table 2.1: Tag descriptions and dimensions. All measurements were made relative to tag orientation when attached to the fish: x indicates maximum rostrum-caudum measurement (mm), y indicates maximum dorsum-ventrum measurement (mm), z indicates maximum proximal-distal measurement (mm). Note that tags B and F contain two sets of values because of a dual-component design.

Tag	Tag type	Mode	Weight (g ± 0.05g)	x (mm ± 0.5mm)	y (mm ± 0.5mm)	z (mm ± 0.5mm)
A	Dart tag	Passive	0.21	84.8	2.0	2.0
B	Petersen disc	Passive	0.73 and 0.64	25.1 and 25.1	25.1 and 25.1	1.0 and 1.0
C	Hexagonal archival logger	Active	4.68	26.1	15.8	7.5
D	Radio tag (laterally compressed)	Active	5.87	29.5 192.1 (antenna)	19.0	13.0
E	Radio tag (laterally compressed)	Active	3.90	24.5 201.0 (antenna)	13.0	7.0
F	Radio tag (cylindrical and applied with backing plate)	Active	7.14 and 1.79	30.5 and 36.0 297.2 (antenna)	14.0 and 11.5	13.0 and 5.0

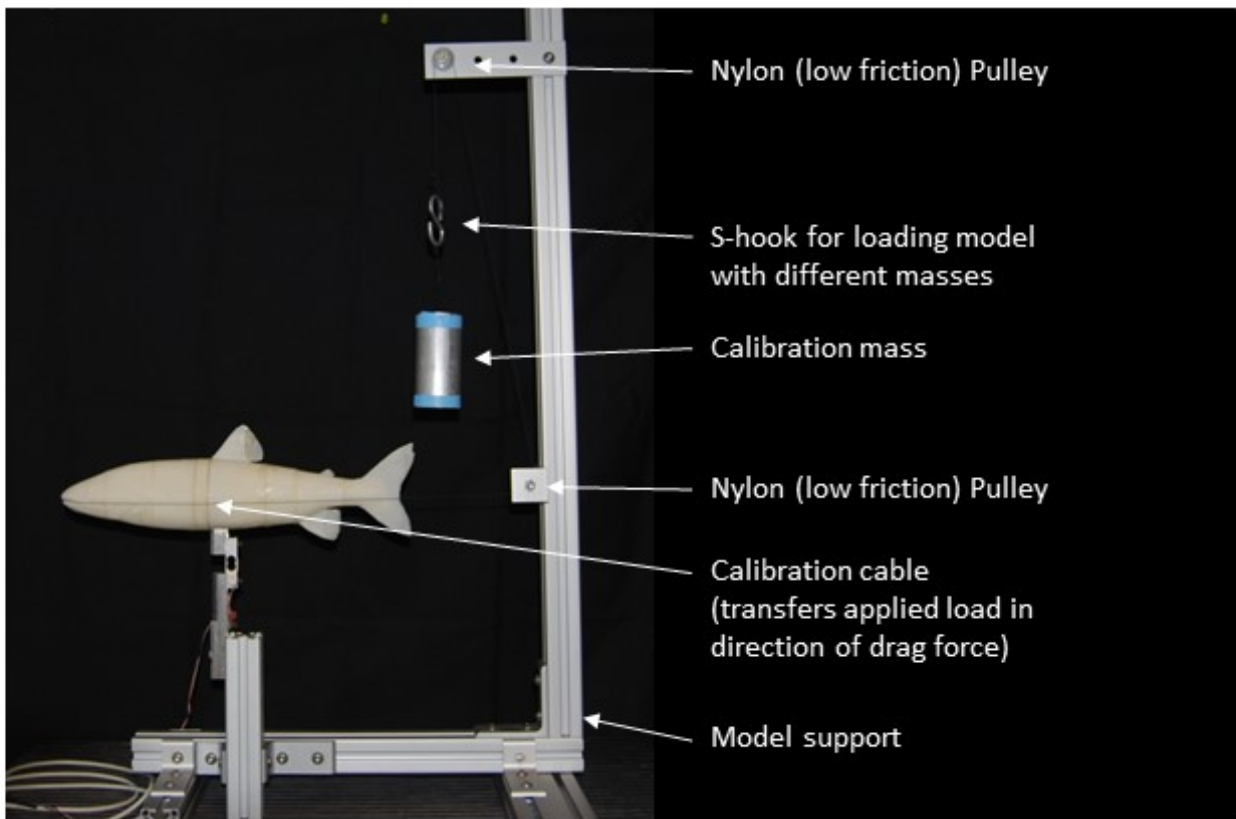


Figure 2.4: Model calibration apparatus. Calibration masses were suspended from a calibration cable under the influence of gravity with pulleys to direct the applied force in the direction of the drag force. Because the calibration mass was suspended vertically, the applied force was simply mass multiplied by acceleration due to gravity (see text for further details).

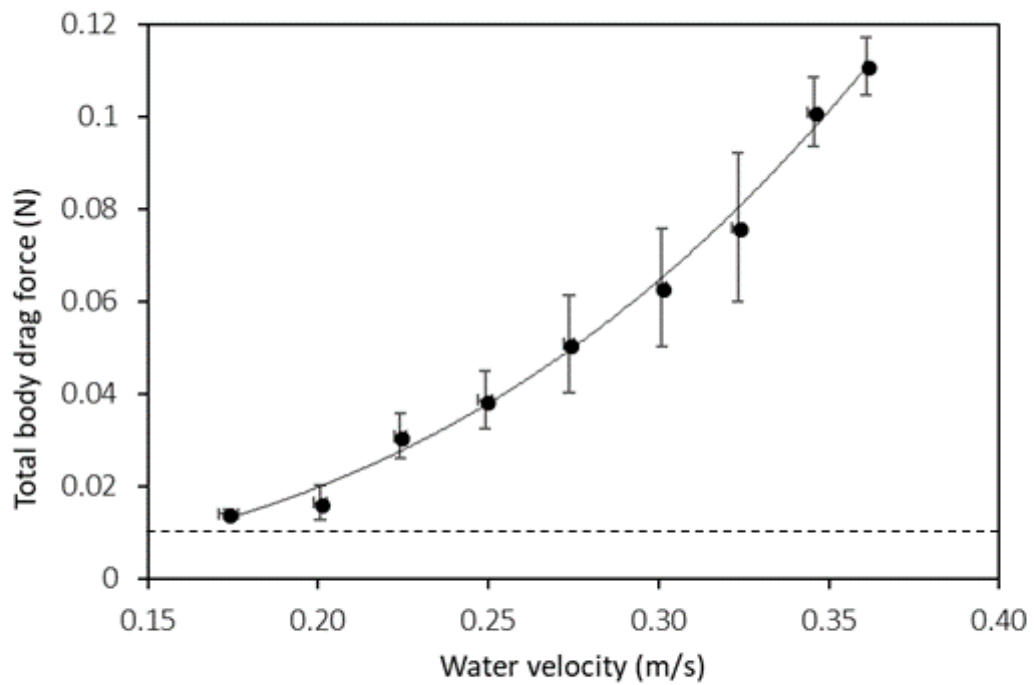


Figure 2.5: Profile drag (N) of the model alone increased as water velocity ($\text{m}\cdot\text{s}^{-1}$) increased. Data are means ($n = 4$) \pm 1 SD. The dashed line indicates the minimum drag force detectable (~ 0.010 N).

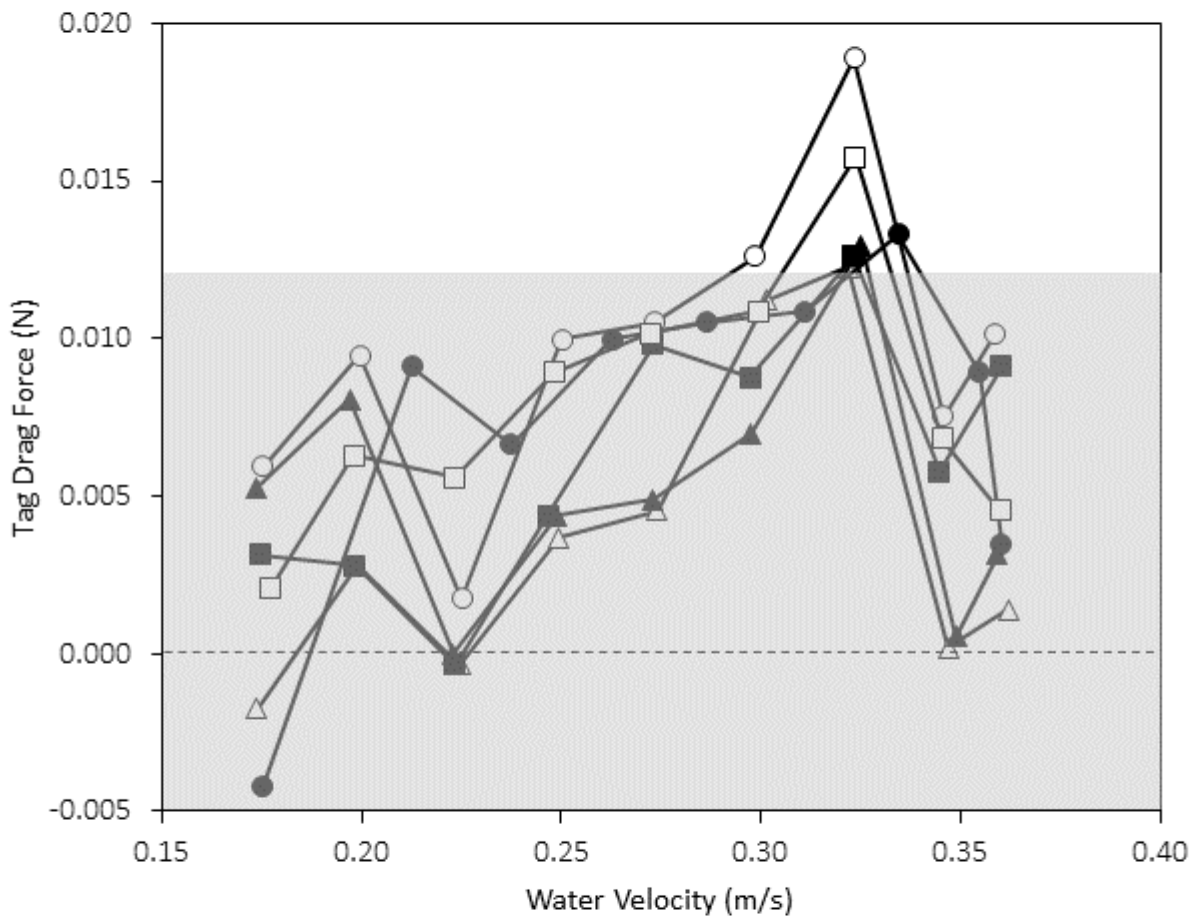


Figure 2.6: Average tag drag (differences in drag measured from model with a tag and without a tag) depict the isolated effect of each tag at stepped water velocity increases. Markers denote each tag as follows: A (Δ), B (\blacktriangle), C (\circ), D (\bullet), E (\square), and F (\blacksquare). Data are the average from two runs in the water tunnel. Note that tag D readings were taken at slightly different velocities due to a switch in personnel operating the water tunnel velocity controls. The dashed line indicates the point at which there is zero tag drag. The confidence interval (grey box) indicates the area in which tag drag cannot be differentiated by instrument noise.

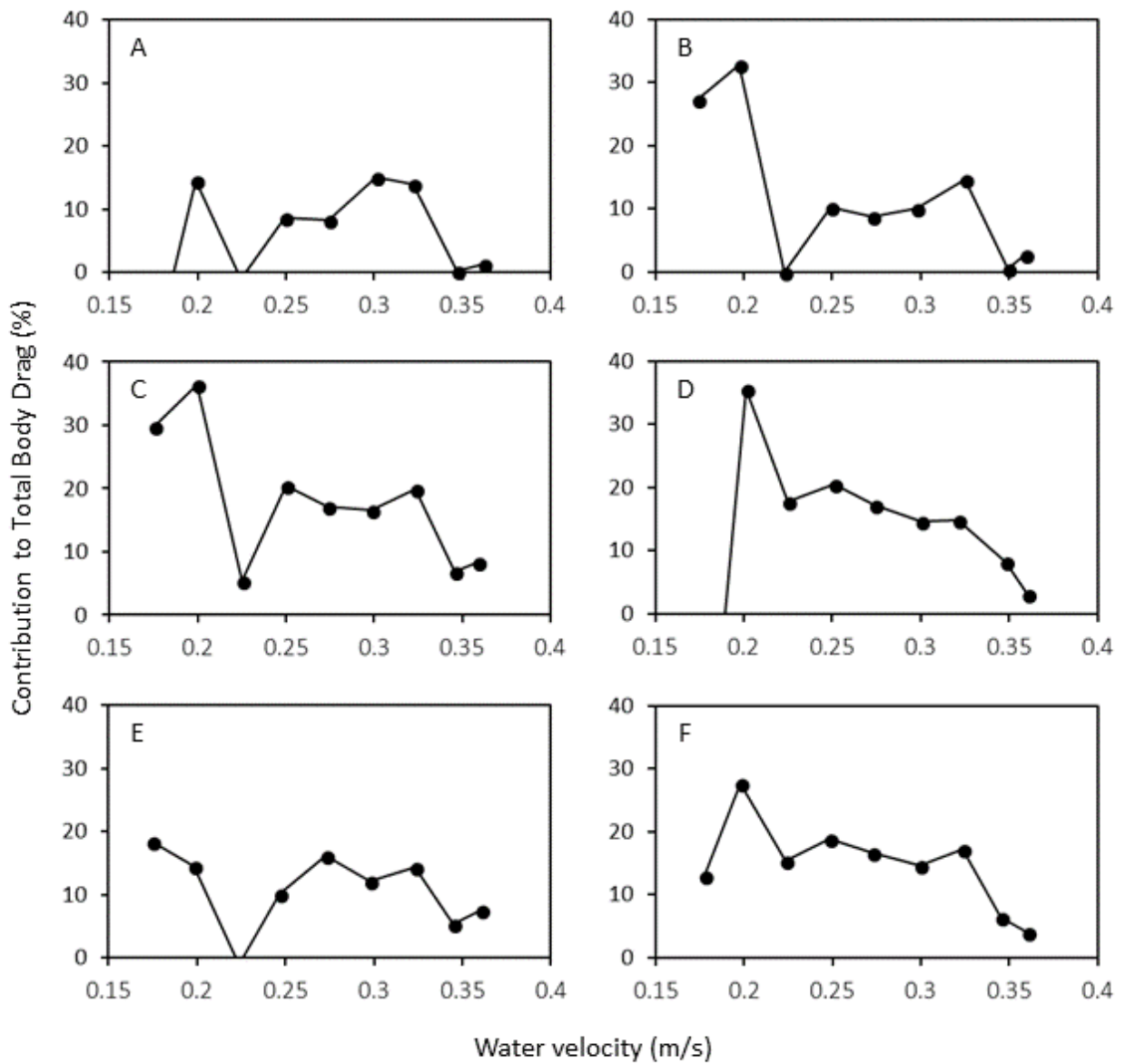


Figure 2.7: Tag drag relative to total body drag (%) at increasing water velocity. Tag drag values and the total body drag are averages.

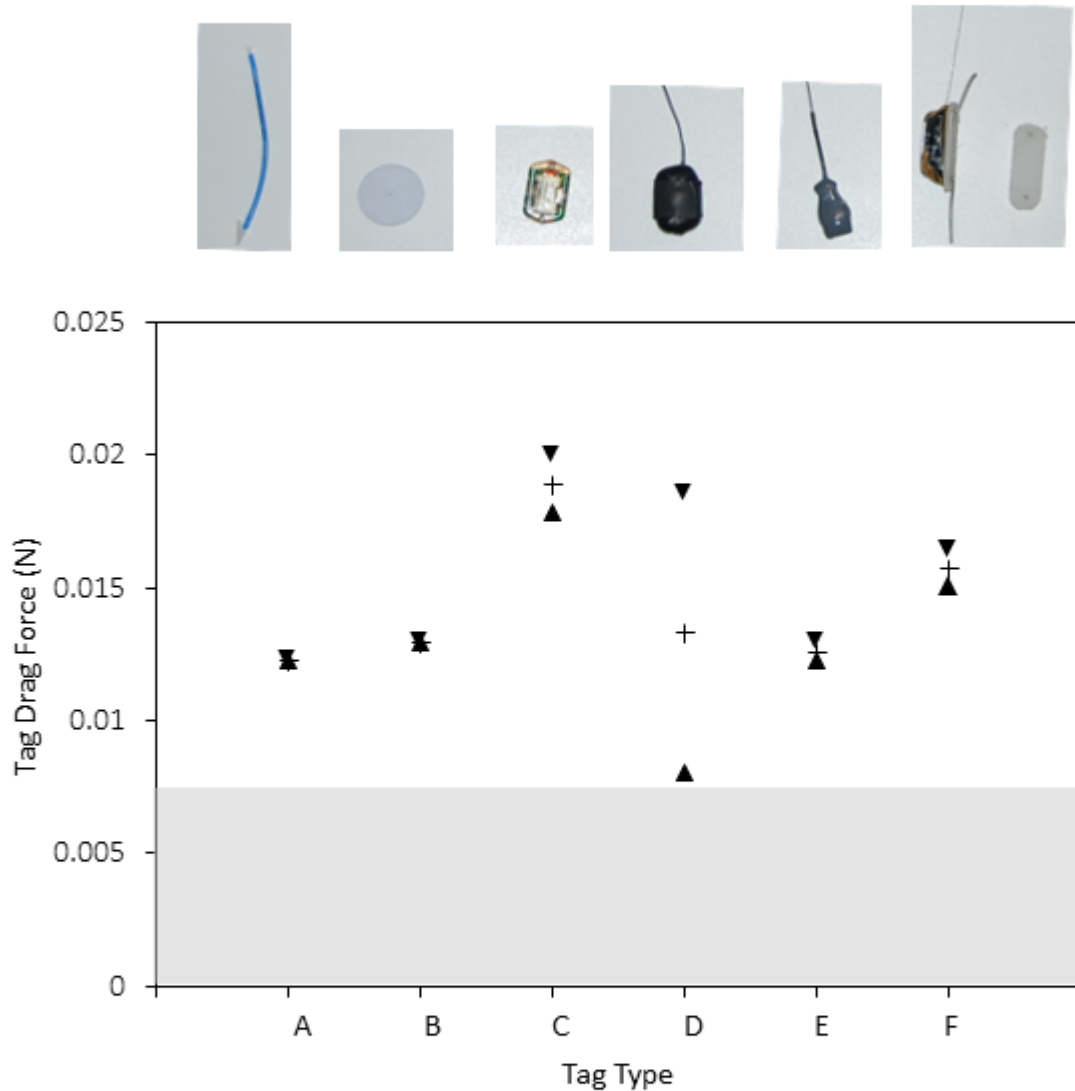


Figure 2.8: Tag drag values for each trial at $0.33 \text{ m}\cdot\text{s}^{-1} \pm 0.005 \text{ m}\cdot\text{s}^{-1}$ water velocity for each tag type (A-F) ($n = 2$). Upper symbol (▼) is maximum drag, lower symbol (▲) is minimum drag, and means are indicated by (+). Tags are arranged in order predicted to be least to most drag inducing (L to R). The confidence interval (grey box) indicates the area in which tag drag cannot be differentiated by instrument noise.

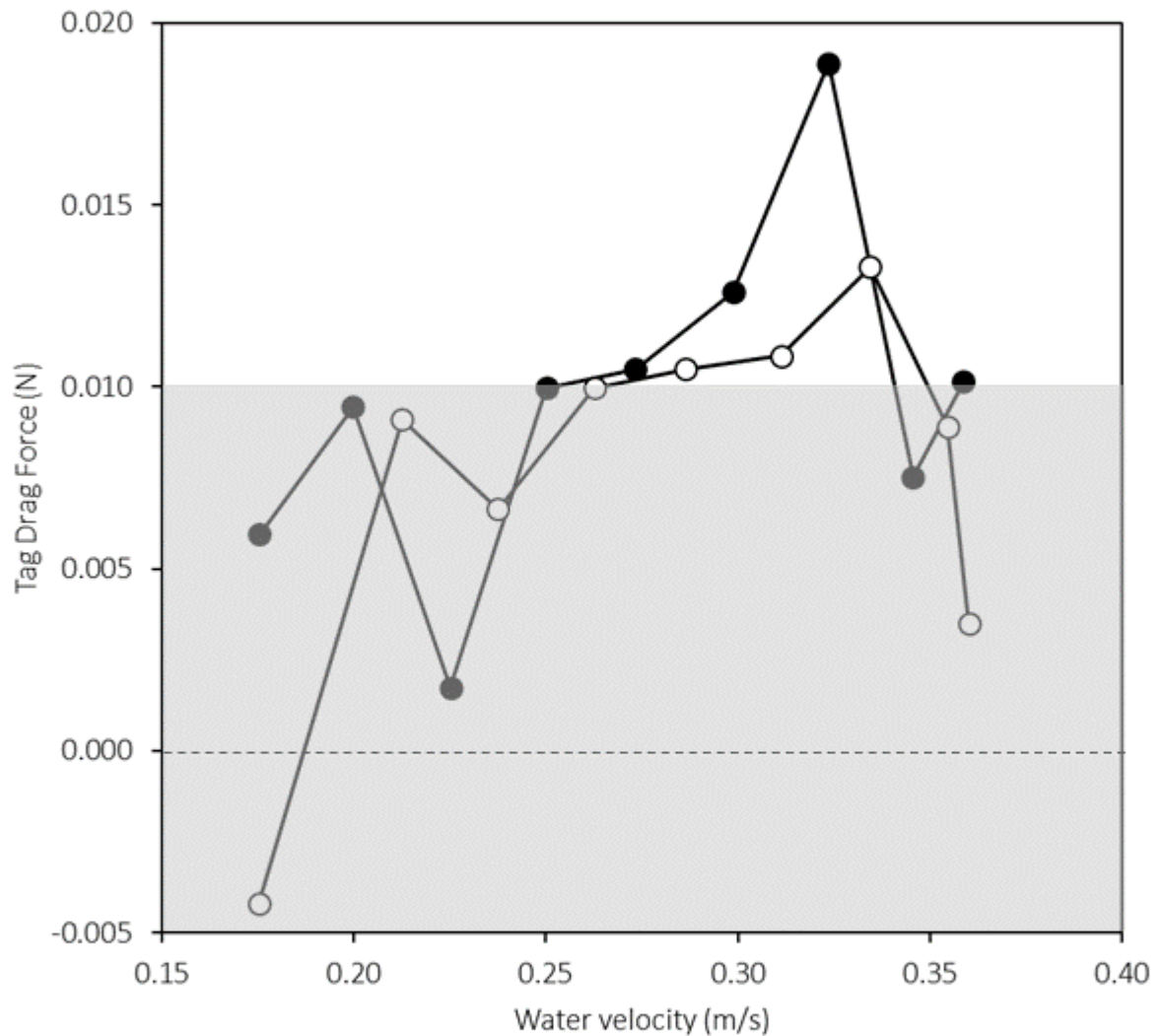


Figure 2.9: Investigating the effect of antenna on tag drag in two tags of comparable surface area and size (C (●) and D (○)). At velocities greater than $0.30 \text{ m}\cdot\text{s}^{-1}$, a tag without an antenna (C) is worse than a tag with antenna (D) for drag induction. The horizontal dashed line represents the point at which the tag drag is zero. The confidence interval (grey box) indicates the area in which tag drag cannot be differentiated by instrument noise.

CHAPTER 3

What makes a tag a drag? A comparative study of the drag effects of varying external fish tag size, shape, and attachment locations on a fusiform teleost fish model.

ABSTRACT

Tags affect behaviour and differ in drag (and presumably cost of transport (COT)). The objectives of this study were to determine how drag is affected by attributes of a tag (size, location of attachment, and shape) and to make recommendations for tag design so as to have minimal impact on a fish. Drag was measured with calibrated load cells fixed to a 3D-printed *Salvelinus namaycush* rigid model in a water tunnel. In order to examine interplay between tag size, shape, and attachment location, nine external tags of three shapes were designed from existing dummy tags and 3D printed in three different sizes (75%, 85%, and 100% of original dummy tag size). These tags were individually affixed to the model at the four different sites and total body drag (profile drag) was measured over stepped increases in water velocity ($0.17 \text{ m}\cdot\text{s}^{-1}$ to $0.37 \text{ m}\cdot\text{s}^{-1}$). Tag attachment resulted in an increase in profile drag as water velocity increased, with most tags producing maximum forces at $0.36 \pm 0.001 \text{ m}\cdot\text{s}^{-1}$. In general, the effects of attachment location on tag drag were highly dependent on tag size and shape, though the

dorsal musculature proximal to the dorsal fin and caudal peduncle attachment sites tended to produce larger drag effects than posterior and anterior dorsal fin attachment sites. The results of this study suggest some criteria to be used as guidelines when designing and/or attaching tags to fusiform teleost fish.

INTRODUCTION

Despite the growing prominence of biotelemetry in fisheries science to study spatial ecology and survival, there is an inadequate understanding of how tag attributes (i.e., tag shape, attachment location, tag size, etc.) affect fish locomotion. All solid objects that move through a fluid environment experience drag forces resulting from interactions between the body and the fluid (air or water) environment (Webb 1971). These drag forces act in opposition to the direction of travel of the object (Webb 1975; Vogel 2013). The presence of an external tag increases the drag experienced by the whole body, regardless of tag design, location of attachment, or size (Thorstad et al. 2013). Increases in profile drag have been linked to increases in cost of transport (COT) (for examples, see Schultz and Webb 2002; Stewart et al. 1983; Tudorache et al. 2014). In order to obtain a clear picture of the precise effect of external tags on survival, the swimming speed, swim mode, and turbulence of water must be considered.

The presence of an external tag may impact profile drag, potentially causing increases in energetic costs, decreasing survival and thus reducing the validity of data obtained from tagged fish (Bannasch 1994; Tudorache et al. 2014). The specific drag effects may differ, as the tags themselves experience drag, which can increase overall drag experienced by the fish. When attached to a fish, the interactions between tag and body shape are predicted to be very complicated.

It can generally be agreed that the smaller the device in proportion to the size of the organism, the less it will impact the organism; however, electronic devices typically present a size-power trade-off. Simply put, the smaller the device, the smaller the battery, the shorter the battery life. Of course, all tags have a minimum size to include the

necessary electronics, but some tags cannot be reduced in size to the same extent as others. In addition to size constraints, the shape of external tags can have a profound influence on profile drag. The tags themselves experience drag, and the degree of streamlining in their shape can dramatically change pressure drag. Currently, few studies have been conducted that focus on identifying these specific drag effects of tags on fish. Of these studies, the majority have been restricted to interpreting tag effects from the comparison between an experimental group and a control group to reduce number of experimental trials (especially for studies using live specimens) (Tudorache et al. 2014). Thus, the scope of these studies is limited and unable to characterize the specific mechanistic effects of various tag attributes (i.e., proximity of tag to body, tag dimensions) without the confounds of individual behaviour.

The objectives of this paper were to identify the effect of variation in external tag attributes (i.e., size, shape, and attachment location) on profile drag using a prototypical teleost fish with fusiform body shape (the lake trout) and to recommend guidelines for tag design and attachments that will produce minimal drag effects. Given that drag cannot accurately be predicted using equations for non-geometric shapes due to the complex interactions of flow characteristics, surface area, and placement on the body, the only way to ascertain drag accurately is through direct measurement (Fox et al. 2006; Webb 1975). In this study, tags of three different shapes were designed (using measurements from dummy tags) and 3D printed in three different sizes (100% of original tag, 85%, and 75%) (Figure 3.1, Table 3.1). These tags were then affixed individually to four attachment sites on a plastic 40 cm fish model, corresponding with commonly-employed

tagging sites (anterior to dorsal fin, in the dorsal muscle proximal to the dorsal fin, posterior to the dorsal fin, and on the caudal peduncle) (Figure 3.1).

Because drag scales to the second power of swimming (or flow) velocity, and in proportion to object size, it was hypothesized that a tag at higher water velocity would produce more drag than one at lower water velocity, and that larger tags would produce more drag than smaller tags (this hypothesis was also tested in the previous chapter). The shape and size of the leading edge were also predicted to affect the magnitude of the tag drag; tags with taller, straight sides on the leading edge may disrupt the boundary layer, producing higher drag forces than more streamlined tags with curved leading edges. In addition, it was expected that the tag on the dorsal fin would have the greatest effect on profile drag, followed by the tag on the caudal peduncle and the tag anterior to the dorsal fin, with the dorsoposterior tag having the least impact. This is due to the assumption of streamline disruption: the dorsal fin cross sectional area would increase significantly with the attachment of a tag, and the caudal peduncle tag would result in a more turbulent wake (Webb 1975). The results of this experiment are intended to inform common practice; identifying aspects of tag design which may have a greater impact on drag, recommending ideal tag designs (i.e., size, shape, attachment location), and providing a basis for future studies using live specimens.

METHODS

In order to characterize effects of varying tag attributes on drag, tags were affixed to a model and tested in a water channel at velocities from $0.17 \text{ m}\cdot\text{s}^{-1}$ to $0.37 \text{ m}\cdot\text{s}^{-1}$. The model creation, load cell mounting and calibration have been described in “Chapter 2: Methods”. The calibration plot for the data presented in this chapter is in the appendix (Figure A2).

Tag creation

To test specific effects of tag size and shape, tag models of three shapes at three scales were created (Figure 3.1, Table 3.1). The tags were modeled from three dummy tags, which were measured using calipers and photographed (with a scale reference). Key measurements included tag length, width, and depth (Table 3.1). 3D models were created in Rhinoceros® 5 from digital photographs, physical tag measurements, and 3D bracket scans (Next Engine® 3D Scanner Ultra HD) (views integrated using Scan Studio™). Tag models were converted to stereolithography files (.STL) and isometrically scaled using MakerBot Print to 100%, 85%, and 75% of original tag measurements. Three tag sizes (small, medium, large) were rendered for each tag shape (cylindrical, laterally compressed disc, laterally compressed), for a total of nine tags (Figure 3.1; Table 3.1). Tags were printed in acrylonitrile butadiene styrene (ABS) plastic using a MakerBot Replicator 2X rapid prototyping printer and the surfaces smoothed after printing using fine grain sandpaper.

Experimental data

For experimental data collection, each tag was placed at one of four attachment locations: directly anterior to the dorsal fin (location 1: 15 cm from snout), on dorsum to

the left of the dorsal fin (location 2: 18 cm from snout), directly posterior to the dorsal fin (location 3: 22 cm from snout), and on the left side of the caudal peduncle (location 4: 33 cm from snout) (Figure 3.1). Each of the nine external tags (Figure 3.1, Table 3.1) were attached individually to each of the four locations with hot glue (Stanley® DualMelt hot-glue, model STHT1-70430) in turn and total body drag measured from $0.17 \text{ m}\cdot\text{s}^{-1}$ to $0.37 \text{ m}\cdot\text{s}^{-1}$. This hot-glue attachment method was assumed not to contribute to the measured drag forces. Control data collection (profile drag values for $0.17 \text{ m}\cdot\text{s}^{-1}$ to $0.37 \text{ m}\cdot\text{s}^{-1}$ water velocity) was repeated four times in total and each experimental test repeated twice.

Data analysis

Control data was used to calculate profile drag (N) of the model on the sting. In order to isolate tag effects, control mean profile drag was subtracted from the mean total body drag values calculated for each tag to provide what has been termed “tag drag.” Measurements of the model without tag attachment, the variation between runs was used to determine the magnitude of a detectable change in drag. Statistics have not been used to analyze the data because multivariate analysis would reduce the confidence of the results given the sample sizes used in this study. However, standard errors for both variables (water velocity and tag drag) have been calculated and are presented in table format in the appendix (Tables A3-A5). In this study, a datum is considered to be different from control measurements if it is greater in magnitude than two standard deviations of the mean drag recorded from the control fish at each velocity. In the figures, this has been presented as a shaded grey bar and referred to as the ‘confidence band.’ Thus, any datum outside this area can be considered a discernable effect of the tag with an acceptable degree of confidence.

RESULTS

Model calibration and control data

A positive correlation was observed between increasing water velocity and increasing measured profile drag of the model without tag attachment (control) (Figure 3.2). Repeated measurements of the model ($n = 4$) in the water tunnel at increasing velocity showed the variation (standard deviation) between runs was, on average, 0.005 N. The minimum drag force detectable by the load cell was 0.010 N (flat dashed line in Figure 3.2); obtained at a water velocity of approximately $0.17 \text{ m}\cdot\text{s}^{-1}$.

Tag drag effects

Tag drag generally increased as flow velocity increased (from $0.17 \text{ m}\cdot\text{s}^{-1}$ to $0.37 \text{ m}\cdot\text{s}^{-1}$). Most tags reached a maximum drag force at $0.36 \pm 0.001 \text{ m}\cdot\text{s}^{-1}$, regardless of tag shape, attachment location, or size (Figure 3.3). When examining individual tag drag values at velocities of $0.36 \pm 0.001 \text{ m}\cdot\text{s}^{-1}$, tag A produced the highest drag for all tag sizes (large: 0.034 N at location 2; medium: 0.028 N at location 2; small: 0.023 N at location 3) (Figure 3.3). Tag C also produced higher drag forces than tag B at the highest recorded velocities for the smallest two tag sizes (medium: 0.019 N at location 2; small: 0.014 N at location 3) (Figure 3.3). Tag B produced the smallest drag effects at flow velocities of $0.36 \pm 0.001 \text{ m}\cdot\text{s}^{-1}$ for the smallest two tag sizes (medium: 0.008 N at location 1; small: 0.004 N at location 4) (Figure 3.3). At full scale, tag B produced higher drag than tag C (respectively, 0.020 N at location 1 and 0.019 N at location 2) (Figure 3.3).

At water velocities of $0.34 \pm 0.003 \text{ m}\cdot\text{s}^{-1}$, location 1 produced the most drag for tags A (medium: 0.017 N and large: 0.019 N) and C (large: 0.013 N) on average (Figure 3.4). Attachment location 2 produced the highest tag drag values for tags A (small: 0.014

N and medium: 0.017 N), B (small: 0.006 N) and C (small: 0.006 N and medium: 0.007 N) (Figure 3.4). Locations 3 and 4 yielded the highest drag value for only one tag: B (large: 0.012 N at location 3; medium: 0.011 N at location 4) (Figure 3.4). With the exception of the smallest size, tag A produced the largest drag effects of all three tag sizes and shapes at any attachment location (Figure 3.4). All values for average velocity, tag drag, and standard errors have been tabulated (Tables A3-A5).

DISCUSSION

The practice of tagging animals for research and data acquisition relies on two main assumptions: the tagging process will not significantly impact survival, and the tag itself will not have any detectable effect on the tagged animal. While data obtained from telemetry and tagging studies are useful across a host of applications (conservation science, aquatic science, etc.), if either assumption has been violated, the validity of the tagging data is called into question. Invalid data may mislead researchers, managers, or decision makers, causing them to come to false conclusions and/or to misguided conservation efforts.

Tag effects refer to any modification in condition, behaviour, or locomotion and are generally difficult to study in isolation when using live specimens (Ross and McCormick 1981). One important tag effect is that of the tag on metabolic cost of transport (COT). A 1994 study conducted by Bannasch and colleagues demonstrated the connection between tag profile optimization and reduction of the effect of the tag on profile drag and swimming energetics of penguins. Their tag design increased profile drag by 15-25% at low speeds ($1.5-2.5 \text{ m}\cdot\text{s}^{-1}$) and 41% at high speeds ($4 \text{ m}\cdot\text{s}^{-1}$). In contrast, unoptimized tags increased profile drag by 52-71% at low speeds ($1.5-2.5 \text{ m}\cdot\text{s}^{-1}$) and 100% at high speeds ($4 \text{ m}\cdot\text{s}^{-1}$) (Bannasch et al. 1994). In addition, the optimized tag reduced metabolic cost by 87% (in comparison with the unoptimized tag) (Bannasch et al. 1994).

The first objective of this paper was to determine the effect of external tag attributes (size, shape, attachment location) on profile drag (as a proxy for COT) of a lake trout. Drag of a rigid model was measured at stepped velocity increases (from $0.17 \text{ m}\cdot\text{s}^{-1}$

to $0.37 \text{ m}\cdot\text{s}^{-1}$) in a water tunnel (Figure 3.2). As hypothesized (and as seen in the previous chapter), increased velocity tended to produce increased tag drag (Figure 3.3). The average drag of 0.108 N at $0.36 \text{ m}\cdot\text{s}^{-1}$, obtained for the 40 cm model alone in this study, is similar to drag values reported in the literature (e.g. 0.080 N at $0.38 \text{ m}\cdot\text{s}^{-1}$ in Webb (1971) for a 30 cm model) (Figure 3.2). Likewise, tag drag for a dangling acoustic tag in a water tunnel has been experimentally measured as approximately 0.006 N at a water velocity of $0.32 \text{ m}\cdot\text{s}^{-1}$ (Arnold and Holford 1978), which is comparable to the tag drag of 0.008 N at $0.32 \text{ m}\cdot\text{s}^{-1}$ observed for several tags and configurations (e.g., small tag B at locations 1 and 2 and medium tag B at locations 2 and 3) in this study (Figure 3.3).

Tag drag was only detectable (outside of instrument noise – shaded regions in data figures) at velocities of $0.30 \text{ m}\cdot\text{s}^{-1}$ or above with two exceptions – the most drag inducing (large tag A) and the least drag inducing (small tag B) (Figure 3.3). In general, as hypothesized, larger tags produced higher tag drag values than smaller tags (Figure 3.3). Of the tags examined in this study, tag A caused the greatest increase in drag force across all sizes and locations, increasing drag on the fish by as much as 29% (large tag at location 4) (Figure 3.3). Tag C produced a maximum detectable drag for all tag sizes, contributing to 16-17% of total body drag (large tag at location 4; medium and small tags at location 2) (Figure 3.3). Tag B was the least drag-inducing of the tags, with only the largest two tags producing detectable tag drag; large tag contributing to 16% of total profile drag at location 1 and the medium tag contributing to 18% of total profile drag at location 4 (Figure 3.3). These results are likely caused by leading edge effects; taller, straighter sides on the leading edge extend the tag away from the body, possibly disrupting the boundary layer and producing higher drag than tags with shorter, curved

leading edges. In addition, leading edges not tight against the fish may induce drag if a more laminar boundary layer were to separate in the space between the tag and the fish body.

As presented in the results, tag size can have a significant impact on drag: for more drag-inducing tags (i.e., tag A), a small decrease in size (e.g. 15-25%) may result in drag force reductions of 15-20%. This is especially relevant for anterior tag placements (location 1); independent of tag shape, a 25% increase in tag size may increase drag by approximately 50% (tag A at $0.17\text{m}\cdot\text{s}^{-1}$) (Figure 3.3).

At water velocities of $0.34 \pm 0.003 \text{ m}\cdot\text{s}^{-1}$, location 1 produced the most drag for the two largest A tags (0.017 N and 0.019 N) and the large C tag (0.013 N) on average (Figure 3.4). As hypothesized, attachment location 2 produced the highest tag drag values for tags A (small: 0.014 N and medium: 0.017 N), B (small: 0.006 N) and C (small: 0.006 N and medium: 0.007 N) (Figure 3.4), indicating that the disruption of streamlining at the dorsal fin is drag-inducing. Locations 3 and 4 yielded the highest drag value for only one tag: B (large: 0.012 N at location 3; medium: 0.011 N at location 4) (Figure 3.4). In contrast, in water velocities between $0.30 \text{ m}\cdot\text{s}^{-1}$ and $0.36 \text{ m}\cdot\text{s}^{-1}$, location 4 produced detectable tag drag ranging from a 29% increase in profile drag (large tag A) to a 12% increase in profile drag (small tag C) for seven of the nine tags (all sizes of tag A, medium tag B, and all sizes of tag C) (Figure 3.4). This is likely due to the wake-inducing nature of posteriorly placed tags (i.e., causing a turbulent boundary layer near the posterior, leading to wake formation) (see Webb 1975 for a detailed description of hydrodynamics, boundary layer flow, and vortex formation).

Tudorache and colleagues (2014) conducted a similar study comparing two tag attachment locations (one at centre of mass and one 0.125 bl from the snout) and tag of three sizes on *Anguilla anguilla* (European eel). The results indicated that tags placed at the centre of mass, a commonly-employed attachment site for tagging eels, caused a 30% decrease in optimal swimming speed (from control) and an elevated COT significantly higher than that of the other attachment location or the control COT (Tudorache et al. 2014). The more rostral tag attachment site also increased COT significantly from the control, but only decreased optimal swimming speed by 15% (Tudorache et al. 2014). The smallest tag (tag drag = 0.05 N) increased COT by 10% while decreasing optimal swimming speed by 10%; the medium tag (tag drag = 0.10 N) increased COT by 18%, decreasing optimal swimming speed by 22%; and the largest tag (tag drag = 0.20 N) increased COT by 40% and decreased optimal swimming speed by over 100% (Tudorache et al. 2014). This suggests it is important to take into account both the swimming mode and morphology of the species to be tagged when designing/affixing tags to fish.

From the results, it can be concluded that, for a 40 cm lake trout in flow velocities of $0.17 \text{ m}\cdot\text{s}^{-1}$ to $0.37 \text{ m}\cdot\text{s}^{-1}$, cylindrical tags (i.e., tag A) are the least desirable (highest energetic costs) – particularly when attached to the musculature proximal to the dorsal fin. Ideally, laterally compressed tags that exhibit rostral-caudal, dorsal-ventral, and proximal-distal symmetry (i.e., tag B) should be used to study lake trout, or similarly-sized fusiform teleost fish. If tags fall within 28 mm x 19 mm x 20 mm (tag B (medium), Table 3.1), the results of this paper suggest that drag effects will be negligible at any attachment location at most flow velocities from $0.17 \text{ m}\cdot\text{s}^{-1}$ to $0.37 \text{ m}\cdot\text{s}^{-1}$ (Figure 3.3).

Regardless of tag size and shape, however, it is advisable to attach tags anterior to the dorsal fin to minimize drag effects likely caused by flow disruption.

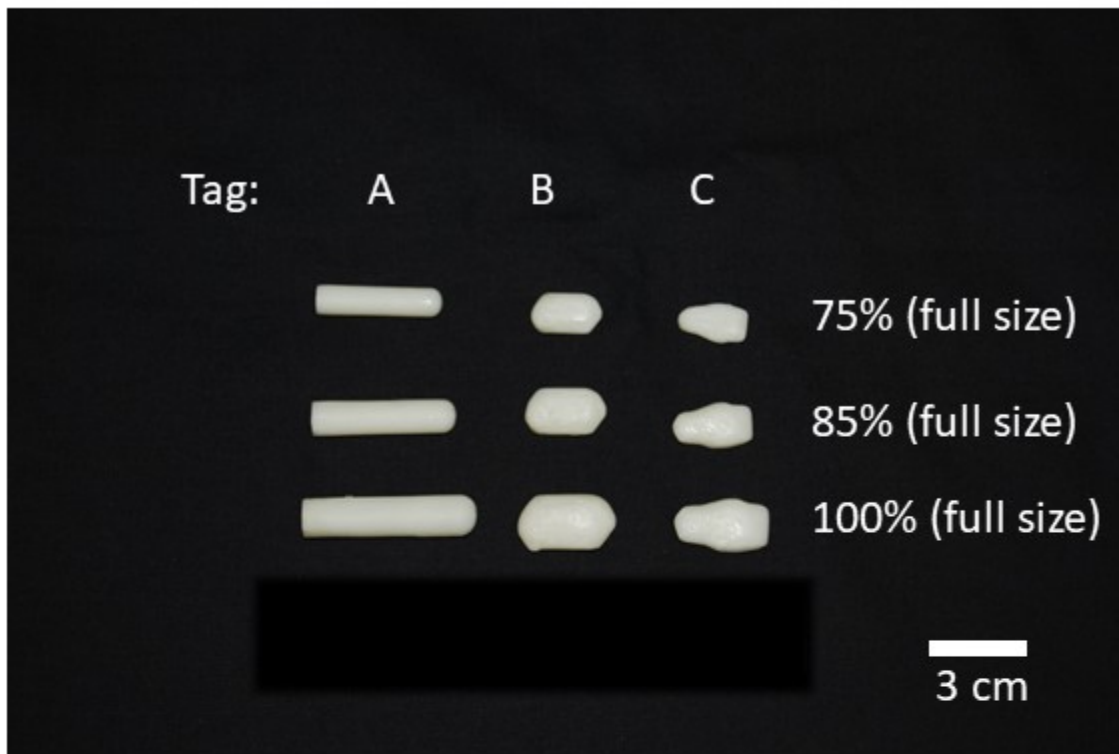
When taking into consideration the importance of streamlining to delay boundary layer separation in carangiform/subcarangiform swimming (employed by lake trout), compact, laterally-compressed tags posterior to the dorsal fin are still the least likely to disrupt the boundary layer (Webb 1971). However, given that the body undulations are most pronounced at the peduncle, and utilized to control wake patterns, it may be that the caudal peduncle tag attachment site is not as drag-inducing in live fish as in rigid models. This is highly dependent on the flow and would likely have more pronounced effects at lower velocities in more laminar flows.

The use of a static model has several advantages and disadvantages, which have been debated and discussed at length in the literature (reviewed in Harris 1938; Schultz and Webb 2002; Webb 1975). However, the real value of using a rigid model is to determine comparative results (experimental condition relative to a control/baseline) that help draw conclusions about overall tag drag trends (Arnold and Holford 1978; Vandenabeele et al. 2015; Webb 1975). In this study, the experimental design and setup allowed for a high degree of repeatability with a low degree of variability (Figure 3.2). Water velocity varied, on average, 1% between runs, and drag force by 17% (when the first drag force value is excluded from standard deviation, drag force variation drops to only 10%) (Figure 3.2). In studies with live fish, it is nearly impossible to achieve such a repeatable experiment across samples due to individual variation (e.g., size, state of health, behaviour) (Dunlop et al. 2010).

The use of a model also allows for a virtually unlimited number of test repetitions, and allows for *ad hoc* adjustments of experimental conditions if unexpected results are obtained during data collection. Thus, without the use of live fish, procedures may be refined, tested, and re-tested, thereby increasing overall fish welfare. Models also produce results that more clearly show biomechanical trends without the confounds of individual variation and behaviour.

The results of this study identify which aspects of tag design and attachment locations may be the most drag-dependent for lake trout in a specific flow regime. These results are designed to be used as a starting point for further studies using live specimens both in the lab and in the field. Future studies should make use of the relevant findings of this paper to test effects of tag attachment location, shape, and size on different fish body types and swimming modes using respirometers, dye flow visualization, and/or electromyogram to more precisely determine tag effects (Jepsen et al. 2005; Jepsen et al. 2015; Thorsteinsson 2002).

Although data obtained from tagging studies have been used in identifying possible sources of fish population declines, and monitoring the effectiveness of conservation efforts, the validity of these data depends on negligible drag effects. However, current studies often neglect the quantification of tag effects (i.e., COT, drag, boundary layer turbulence or separation, tag-induced behaviours) and, by extension, produce results with questionable validity. It is the responsibility of researchers and scientists to broaden understanding of tag effects in order to design tags that will minimally impact the condition of the tagged animal, providing data which more accurately reflects the general, untagged population.



Attachment Location

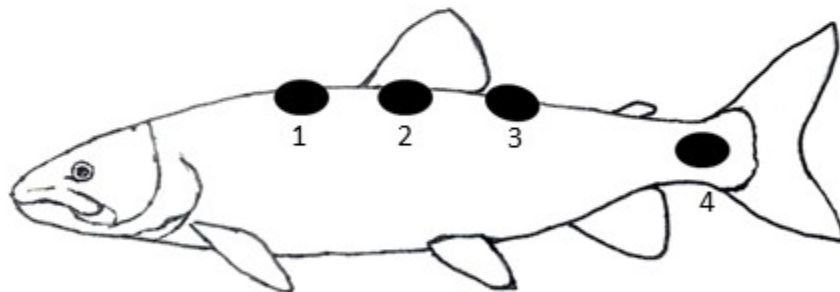


Figure 3.1: Nine 3D printed tags used for this study: three model tag types of three sizes (Top). Line drawing of a *Salvelinus namaycush* with the four attachment locations used in this study. From anterior to posterior: Location 1 (anterior to dorsal fin), Location 2 (musculature proximal to dorsal fin), Location 3 (posterior to dorsal fin), Location 4 (caudal peduncle) (Bottom).

Table 3.1: Tag descriptions and dimensions. All measurements were made relative to tag orientation when attached to the fish: x indicates maximum rostrum-caudum measurement (mm), y indicates maximum dorsum-ventrum measurement (mm), z indicates maximum proximal-distal measurement (mm).

Tag	Tag shape	Length (mm ± 0.05mm)	Width (mm ± 0.05mm)	Depth (mm ± 0.05mm)
A (75%)	Cylindrical	39.52	9.67	9.67
A (85%)		44.78	10.96	10.96
A (100%)		52.69	12.90	12.90
B (75%)	Laterally compressed	22.96	15.72	16.36
B (85%)	disc	27.59	18.90	19.66
B (100%)		32.46	22.23	23.13
C (75%)	Laterally compressed	18.44	11.02	6.55
C (85%)		26.01	15.55	9.24
C (100%)		30.60	18.29	10.87

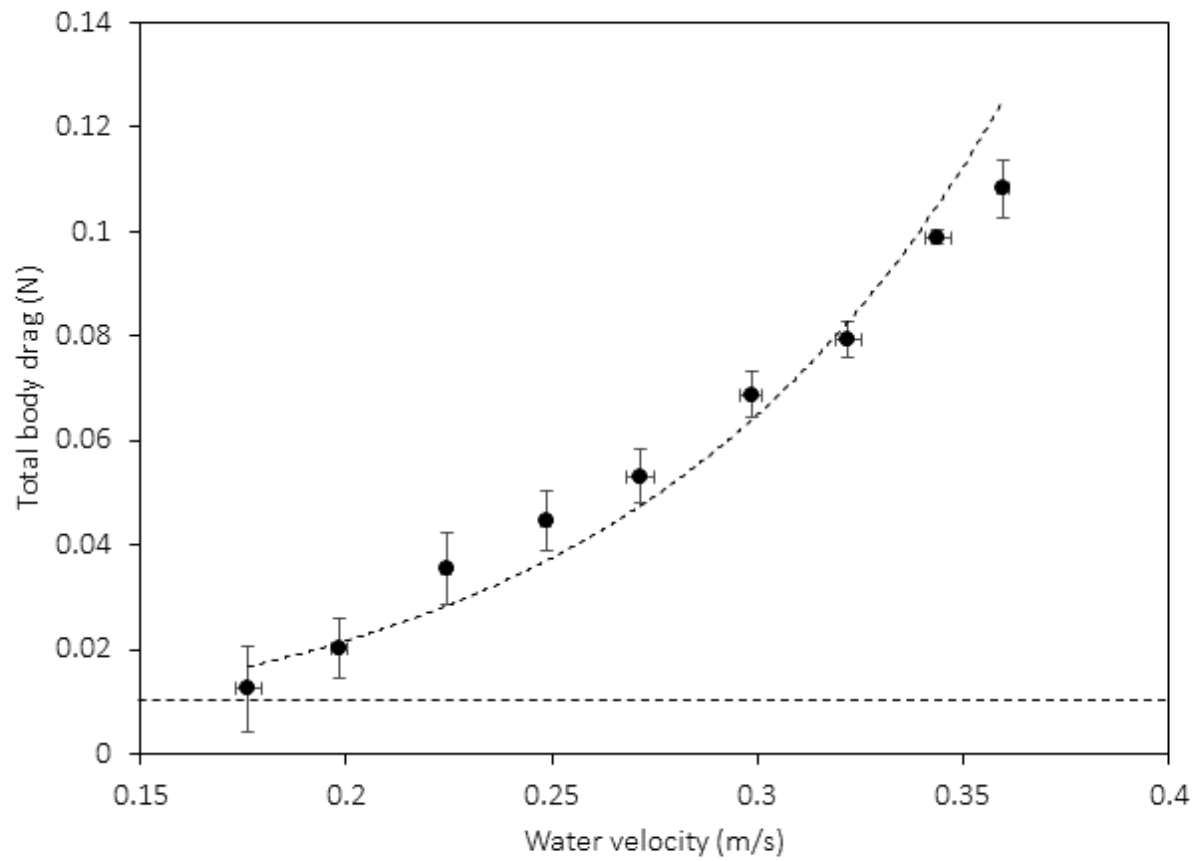


Figure 3.2: Profile drag (N) of the model alone increased as water velocity ($\text{m}\cdot\text{s}^{-1}$) increased. Data are means ($n = 4$) \pm 1 SD. The dashed line indicates the minimum drag force detectable (~ 0.010 N).

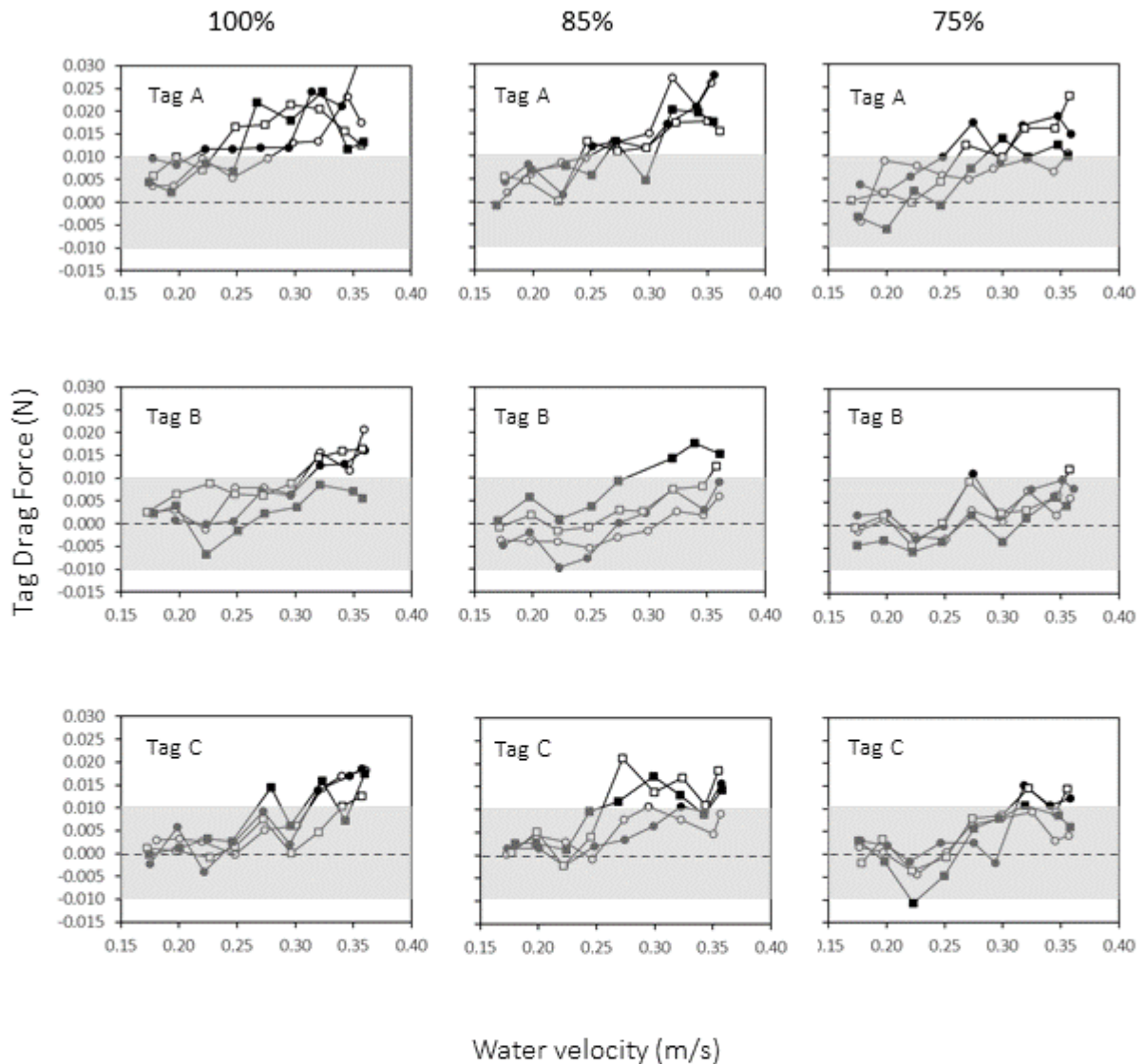


Figure 3.3: Average tag drag (differences in drag measured from model with a tag and without a tag) depicts the isolated effect of each tag shape, size, and attachment location at stepped water velocity increases. Markers denote each attachment location as follows: Location 1 (\circ), Location 2 (\bullet), Location 3 (\square), and Location 4 (\blacksquare). Data are the average from two runs in the water tunnel. Confidence bands (in grey) indicate ± 0.010 N (2 SD). Dashed lines indicate a zero percent contribution of the tag to profile drag.

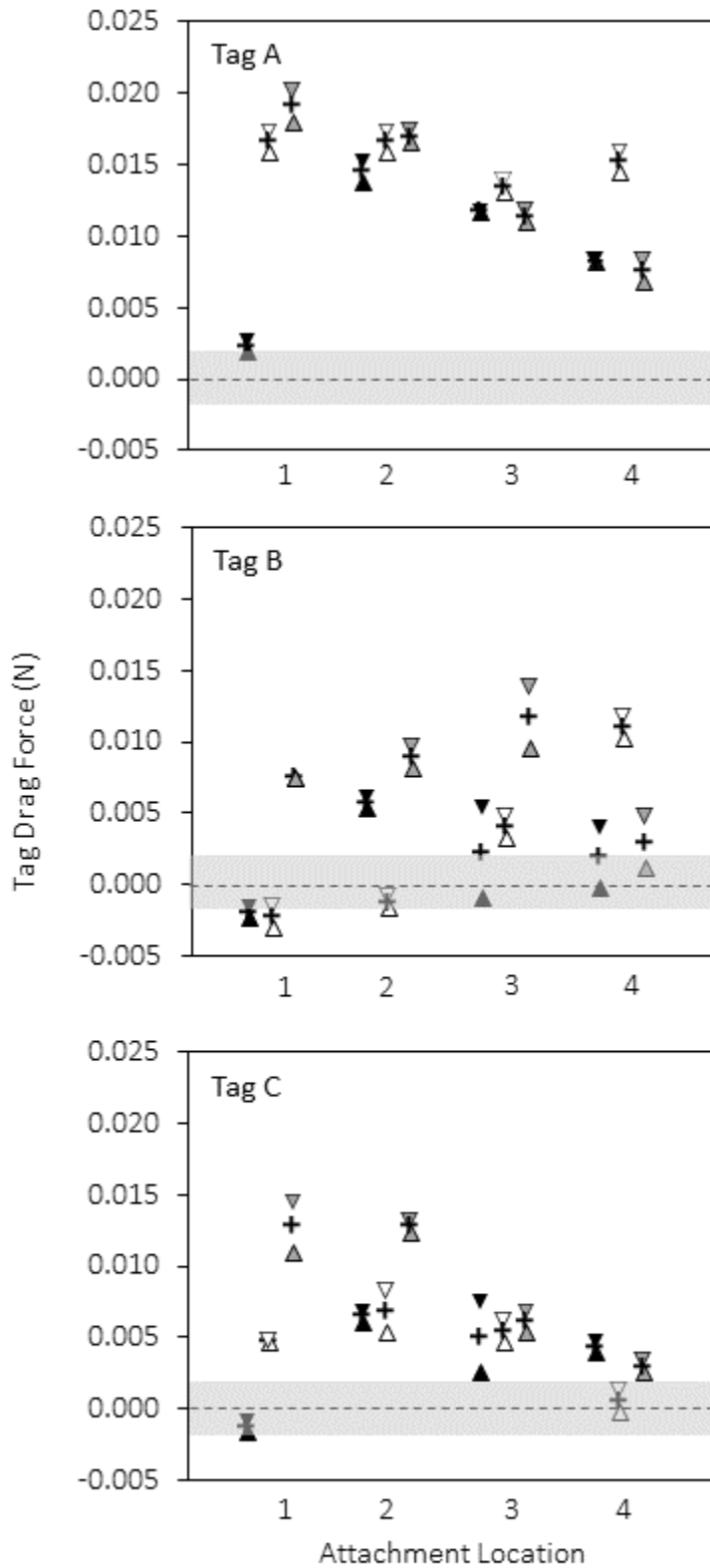


Figure 3.4: Tag drag values at $0.34 \pm 0.003 \text{ m}\cdot\text{s}^{-1}$ for all tags. Average tag drag is indicated by (+); lowest readings by (▲) for the 75% scale tags, (△) for the 85% scale tags, and (▲) for the 100% scale tags; and highest readings by (▼) for the 75% scale tags, (▽) for the 85% scale tags, and (▽) for the 100% scale tags. Confidence bands (in grey) indicate $\pm 0.002 \text{ N}$ (2 SD). Dashed lines indicate the point at which tag effect is zero.

CHAPTER 4

General Discussion

The objectives of this thesis were to describe drag effects of external tags already in existence and commonly used in the field, and to identify and characterize the effects of systematic variation of tag attributes (tag shape, size, and attachment location). From these results, guidelines were proposed for tag size, shape, and attachment sites that would produce minimal tag drag on a fusiform teleost fish. This is the first study to use 3D printed models (fish and tags) in a water tunnel to classify drag affects of specific tag attributes and attachment locations.

When commonly-employed external tags were affixed to an attachment location often used for external tag attachment (musculature proximal to the dorsal fin), an increase in tag drag was seen with increasing flow velocities, as expected (Chapter 2). The tags that produced the greatest drag were the tags that protruded furthest from the fish body (i.e., the least streamlined). The most drag-inducing tag (hexagonal archival logger) did not have an antenna to potentially increase drag (see Murchie et al. 2004), nor the largest total surface area of all the tags being tested, but straight, tall, leading edges appeared to have disrupted the streamlining of the model. The tags that produced lesser tag drag were ones with a more laterally compressed, streamlined design. Specifically,

the size of the leading edge appeared to have an impact on the magnitude of tag drag (i.e., smaller, curved leading edges induced less drag). This postulation would need to be confirmed with dye flow visualization (available in most water tunnels, but difficult to properly implement) to determine the nature and extent of the flow disturbance. Particle image velocimetry could also be used to quantitatively measure the flow of fluid over and around the surface of the fish (also difficult to use and requires expensive equipment). However, from the results, tag shape appears to be more of a factor in drag induction than size.

When a more systematic approach was taken (Chapter 3) (varying tag type, size, and attachment location), tag drag values also increased with increasing water velocity. Larger tag size did not always correspond with higher drag values. Rather, the cylindrical tag produced the highest tag drag across all attachment locations and tag sizes. The other two tag shapes produced much lower tag drag values and larger tags generally produced larger drag values. Of the three shapes, the laterally compressed disc shaped tag produced nearly undetectable drag across all water velocities used in this study, tag sizes, and attachment locations. Again, this compliments the data from chapter 2 and points to the role of shape in determining drag effects. It also suggests the importance of a streamlined leading edge, as the tag with the smallest tag drag (tag B) had a maximum depth larger than the other two tags at all scales. However, this disc shaped tag lay flush with the dorsum when attached to the fish, and the edges were tapered (the depth reported in Table 3.1 was measured from the middle of the tag).

Of the four attachment locations, as predicted, the tag on the musculature of the dorsum proximal to the dorsal fin produced the most drag across a range of tag shapes

and sizes. The caudal peduncle also produced higher drag values for the majority of the tags. This highlights the importance of streamlining and the maintenance of a laminar boundary layer in drag reduction. Laterally placed tags may disrupt streamlining and create turbulence in the boundary layer, possibly increasing profile drag. If the increase in drag is due to a turbulent boundary layer, it could be verified using dye flow visualization. Thus, the ideal tag for a fusiform teleost would be a laterally compressed disc shape at any location (for the range of test velocities) within the given dimensions: 28 mm x 19 mm x 20 mm, or a laterally compressed tag immediately posterior to the dorsal fin on the dorsum. Cylindrical tags should be avoided, especially when attached laterally (i.e., proximal to the dorsal fin or on the caudal peduncle).

It is also important to note that the attachment method used in these experiments (hot glue affixing the tag to the model) produced a virtually seamless connection between tag and model. This is especially relevant at the leading edge, where streamlining is key to maintaining drag reduction. When tagging live fish, the tag attachment technique should strive to maintain a tight connection between the tag and the body of the fish, particularly at the leading edge. It is likely that any gaping between the body and the tag would cause the tag to pull away from the body at higher water velocities, thereby increasing surface area, profile drag, (and potentially cost of transport).

There was a unique point very distinctly identified in chapter 2 that was described as a “resonance frequency” and ascribed to the mechanical interaction between model, water flow velocity, and test section dimensions. At this velocity ($0.22 \text{ m}\cdot\text{s}^{-1}$), drag values were consistently lower than expected, deviating from the observed trends. In chapter 3, this effect was faintly visible, but given the noise of the data, it was not as readily

apparent as in chapter 2. Another difference between the chapters was that tag drag values reached maximum levels at approximately $0.33 \text{ m}\cdot\text{s}^{-1}$ in chapter 2, but in chapter 3, most tags reached peak tag drag at the highest testing flow velocity ($\sim 0.36 \text{ m}\cdot\text{s}^{-1}$). This may have been due to the effect of different attachment locations in chapter 3 creating differences in the flow over the body relative to chapter 2 as velocity increased.

One of the most unique aspects of this research is its novel use of technology (3D modeling and printing). Very few studies have taken advantage of 3D modeling and printing to answer a biological question (Beaumont et al. 2017; Lind et al. 2017; Pavlov and Rashad 2012). Of these studies, the majority have used 3D modeling in biomedical research, rather than in ecological applications (Campos et al. 2015). While there have been several popular press articles about the use of 3D printing to solve ecological problems, these experiments have yet to be published in a peer-reviewed journal.

In ecological research, printed models allow for a high degree of control over variables including organism size, maturity, and tag attachment sites. Measurements of specimens (living or preserved) exhibiting desirable characteristics (defined by the focus of the study) may be used to model an ideal specimen for research. For example, if juveniles are the target specimens, juvenile models can be designed, printed, and used for an indefinite period without the confounding effects of development.

The use of models also allows for much greater ease and accuracy of repeatability than using live or preserved organisms. Additionally, the use of models over preserved specimen is preferable because preserved specimen do not produce the same body undulations as live fish (Wu 1977, cited in Daniel 1981). Use of a preserved specimen is not only restricted by the inevitable decomposition of the specimen, but studies that have

used tow tanks and preserved specimen have observed drag values higher than predicted in live fish (Webb 1978, cited in Daniel 1981). Whilst rigid models may lack drag-reducing mechanisms such as flexible bodies, mucous layers, or the ability to use a wake to generate thrust, they provide a method to accurately determine drag (being directly affixed to a sting containing a strain gauge) for an indefinite period of time. Thus, profile drag values obtained from testing with a rigid model are expected to be higher than profile drag experienced by live fish, but they allow for demonstration of drag-induction trends through comparative profile drag between experimental and control conditions.

Future studies should incorporate different fish body forms and swimming modes, testing tag drag effects on models to determine an ideal design for the species being tagged. The addition of dye flow visualization would illuminate the potential effects of tags on streamlining and boundary layer turbulence. Once dye flow visualizations and drag effects have been determined, tags designed to reduce drag effects should be tested on live specimens. The implications of this research reach beyond tagging fish to other species and provide the opportunity to design tags that have been experimentally verified to produce negligible drag effects and preserve the validity of tagging data.

LITERATURE CITED

- Alexander, DE (1990) Drag Coefficients of Swimming Animals: Effects of Using Different Reference Areas. *Biological Bulletin*, 179(2): 186-90.
- Arnold, GP, and Holford, BH (1978) The physical effects of an acoustic tag on the swimming performance of plaice and cod. *Journal du Conseil International pour l'Exploration de la Mer*, 38: 189–200.
- Bannasch, R, Wilson, RP and Culik, B (1994) Hydrodynamic aspects of design and attachment of a back-mounted device in penguins. *J. Exp. Biol*, 194: 83-96.
- Barrett, DS, Triantafyllou, MS, Yue, DKP, Grosenbaugh, MA and Wolfgang, MJ (1999) Drag reduction in fish-like locomotion. *J. Fluid Mech.* 392: 183-212.
- Beaumont, TM, Caldeira Ideias, P, Rimlinger, M, Broggio, D and Franck, D (2017) Development and test of sets of 3D printed age-specific thyroid phantoms for ¹³¹I measurements. *Phys Med Biol*, 14: DOI: 10.1088/1361-6560/aa6514.
- Blake, RW (1983) *Fish Locomotion*. Cambridge University Press: Cambridge, UK. 54-119.
- Bridger, CJ and Booth, RK (2003) The Effects of Biotelemetry Transmitter Presence and Attachment Procedures on Fish Physiology and Behaviour. *Reviews in Fisheries Science*, 11(1): 13-34.
- Broell, F, Burnell, C, and Taggart, CT (2016) Measuring abnormal movements in free-swimming fish with accelerometers: implications for quantifying tag and parasite load. *J. Exp. Biol.*, 219: 695-705.
- Brown, RS, Cooke, SJ, Anderson, WG and McKinley, RS (1999) Evidence to challenge the “2% rule” for biotelemetry. *North Am. J. Fish. Mgmt.*, 19: 867-871.
- Campos, EO, Bradshaw, HD and Daniel, TL (2015) Shape matters: corolla curvature improves nectar discovery in the hawkmoth *Manduca sexta*. *Fundamental Ecology*, 29(4): 462-8.
- Cooke, SJ, Hinch, SG, Wikelski, M, Andrews, RD, Kuchel, LJ, Wolcott, TG and Butler, PJ (2004) Biotelemetry: a mechanistic approach to ecology. *Trends in ecology and evolution*, 19(6): 334-343.
- Cooke, SJ, Hinch, SG, Lucas, MC and Lutcavage, M (2012) Chapter 18 – Biotelemetry and biologging. Pages 819-860 in A. V. Zale, D. L. Parrish, and T. M. Sutton,

- editors. Fisheries Techniques, Third Edition. American Fisheries Society, Bethesda, Md.
- Cooke, SJ, Midwood, JD, Thiem, JD, Klimley, P, Lucas, MC, Thorstad, EB, Eiler, J, Holbrook, C and Ebner, BC (2013) Tracking animals in freshwater with electronic tags: past, present and future. *Animal Biotelemetry*, 1(5): DOI: 10.1186/2050-3385-1-5.
- Daniel, TL (1981) Fish mucus: *In situ* measurements of polymer drag reduction. *Bio. Bull*, 160: 376-382
- Drenner, SM, Clark TD, Whitney, CK, Martins, EG, Cooke, SJ and Hinch, SG (2012) A synthesis of tagging studies examining the behaviour and survival of anadromous salmonids in marine environments. *PLoS One*, 7: e31311.
- Dunlop, ES, Milne, SW, Ridgway, MS, Condiotty, M, and Higginbottom, I (2010) *In situ* swimming behavior of lake trout observed using integrated multibeam acoustics and biotelemetry. *Transactions of the of the American Fisheries Society*, 139: 420-432.
- Fish, FE (1992) Aquatic locomotion. In: *Mammalian Energetics: Interdisciplinary Views of Metabolism and Reproduction* (T. E. Tomasi and T. H. Horton, eds.). Cornell University Press, Ithaca, 34-63 pp.
- Fox, RW, McDonald, AT, and Pritchard, PJ (2006) *Introduction to Fluid Mechanics* (6th ed.) John Wiley and Sons, Inc.
- Frost, DA, McComas, RL and Sandford, BP (2010) The Effects of a Surgically Implanted Microacoustic Tag on Growth and Survival in Subyearling Fall Chinook Salmon. *Transactions of the American Fisheries Society*, 139(4): 1192-1197.
- Gutema, TM (2015) Wildlife Radio Telemetry: Use, Effect and Ethical Consideration with Emphasis on Birds and Mammals. *IJSBAR*, 24(2): 306-13.
- Harris, JE (1938) The roles of the fins in the equilibrium of the swimming fish. *J. Exp. Biol*, 15: 32-47.
- Hubbs, CL and Lagler, KF (2004) *Fishes of the Great Lakes Region* (rev. ed. GR Smith). The University of Michigan Press: Ann Arbor, MI. 44-47, 162-71.

- Jacobson, JA and Hansen, PA (2004, September) Conventional methods in stock identification: internal and external tags. Presented at the 2004 ICES ASC in Vigo, Spain.
- Jadot, C (2003) Comparison of two tagging techniques for *Sarpa salpa*: external attachment and intraperitoneal implantation. *Oceanologia Acta*, 26: 497-501.
- Jepsen, N, Schreck, C, Clements, S and Thorstad, EB (2005) A brief discussion on the 2% tag/bodymass rule of thumb. In: *Aquatic telemetry: advances and applications*. Proceedings of the Fifth Conference on Fish Telemetry held in Europe, Ustica, Italy, 9-13 June 2003 (editors Spedicato, MT, Lembo, G and Marmulla, G). FAO/COISPA, Rome, pp. 255-259.
- Jepsen, N, Thorstad, EB, Havn, T and Lucas, MC (2015) The use of external electronic tags on fish: an evaluation of tag retention and tagging effects. *Animal Biotelemetry*, 3(49): DOI: 10.1186/s40317-015-0086-z.
- Jones, R (1979) Material and methods used in marking experiments in fisheries research. FAO (Food and Agriculture Organization of the United Nations) Fisheries Technical Paper 190, Rome.
- Jones, TT, Bostrom, BL, Carey, M, Imlach, B, Mikkelsen, J, Ostafichuk, P, Eckert, S, Opay, P, Swimmer, Y, Seminoff, JA and Jones, DR (2011) Determining transmitter drag and best-practice attachment procedures for sea turtle biotelemetry. NOAA Technical Memorandum NMFS-SWFSC-480.
- Johnson, MW, Diamond, SL, and Stunz, GW (2015) External Attachment of Acoustic Tags to Deepwater Reef Fishes: an Alternate Approach When Internal Implantation Affects Experimental Design, *Transactions of the American Fisheries Society*, 144:4, 851-859.
- Kölzsch, A, Neefjes, M, Barkway, J, Müskens, GJDM, van Langevelde, F, de Boer, WF, Prins, HHT, Cresswell, BH and Nolet, BA (2016) Neckband or backpack? Differences in tag design and their effects on GPS/accelerometer tracking results in large waterbirds. *Animal Biotelemetry*, 4(13): doi: 10.1186/s40317-016-0104-9.
- Lefrançois, C, Odion, M, and Claireaux, G (2001) An experimental and theoretical analysis of the effect of added weight on the energetics and hydrostatic function

- of the swimbladder of European sea bass (*Dicentrarchus labrax*). *Marine Biology*, 139: 13-17.
- Lind, JU, Busbee, TA, Valentine, AD, Pasqualini, FS, Yuan, H, Yadid, M, Park, SJ, Kotikian, A, Nesmith, AP, Campbell, PH, Vlassa,k JJ, Lewis, JA and Parker, KK (2017) Instrumented cardiac microphysiological devices via multimaterial three-dimensional printing. *Nat Mater*, 16: 303-8.
- Lucas, MC and Baras, E (2000) Methods for studying spatial behaviour of freshwater fishes in the natural environment. *Fish and Fisheries*, 1(4): 283-316.
- Maddock, L, Bone, Q and Rayner, JMV (ed.) (1994) *Mechanics and physiology of animal swimming*. Cambridge University Press: Cambridge, GB. 27-61, 75-124.
- Mech, LD (1983) *A Handbook Of Animal Radio-tracking*. University of Minnesota Press: Minneapolis, MN. 10-12.
- Muir, AM, Bronte, CR, Zimmerman, MS, Quinlan, HR, Glase JD and Krueger, CC (2014) Ecomorphological Diversity of Lake Trout at Isle Royale, Lake Superior. *Transactions of the American Fisheries Society*, 143(4): 972-987.
- Murchie, KJ, Cooke, SJ, and Schreer, JF (2004) Effects of radio-transmitter antenna length on swimming performance of juvenile rainbow trout. *Ecology of Freshwater Fish*, 13: 312-316.
- Nielsen, LA (1992) *Methods of marking fish and shellfish*. American Fisheries Society Special Publication, 23.
- Parker, NC, Giorgi, AE, Heidinger, RC, Douglas, DJ, Prince, ED and Winans, GA (1990) Fish-marking techniques. *American Fisheries Society Symposium* 7: 879 pp.
- Pavlov, VV and Rashad, AM (2012) A non-invasive dolphin telemetry tag: Computer design and numerical flow simulation. *Marine Mammal Science*, 28(1): E16-17.
- Preston-Thomas, H, Turnbull, LG, Green, E, Dauphinee, TM and Kaira, SN (1960) An absolute measurement of the acceleration due to gravity at Ottawa. *Can. J. Phys.*, 38: 824-852.
- Ross, MJ and McCormick, JH (ed.) (1981) *Effects of External Radio Transmitters on Fish*. *Prog. Fish Cult.*, 43(2): 67-72.
- Schultz, WW and Webb, PW (2002) Power requirements of swimming: do new methods resolve old questions? *Integrative and Comparative Biology*, 42(5): 1018–1025.

- Shadwick, RE and Lauder, GV (2006) Fish Biomechanics (Fish Physiology, v.23) (ed. DJ Randall and AP Farrell). Elsevier Academic Press: San Diego, CA. 225-460.
- Stewart, DJ, Weininger, D, Rottiers, DV, and Edsall, TA (1983) An energetics model for lake trout, *Salvelinus namaycush*: application to the Lake Michigan population. Canadian Journal of Fisheries and Aquatic Sciences, 40: 681–698.
- Thorstad, EB, Rikardsen, AH, Alp, A and Økland, F (2013) The Use of Electronic Tags in Fish Research – An Overview of Fish Telemetry Methods. Turkish Journal of Fisheries and Aquatic Sciences, 13: 881-96.
- Thorsteinsson, V (2002) Tagging Methods for Stock Assessment and Research in Fisheries. Report of Concerted Action FAIR CT.96.1394 (CATAG). Reykjavik. Marine Research Institute Technical Report, 79: 1-183.
- Tudorache, C, Burgerhout, E, Brittijn, S and van den Thillart, G (2014) The Effect of Drag and Attachment Site of External Tags on Swimming Eels: Experimental Quantification and Evaluation Tool. PLoS ONE, 9(11): e112280.
- Vandenabeele, SP, Shepard, ELC, Grémillet, D, Butler, PJ, Martin, GR and Wilson, RP (2015) Are bio-telemetric devices a drag? Effects of external tags on the diving behaviour of great cormorants. Marine Ecology Progress Series, 510: 239-49.
- Vickery, BJ, and Watkins, RD (1964) Flow induced vibrations of cylindrical structures. In: Hydraulics and Fluid Mechanics: Proceedings of the First Australasian Conference Held at the University of Western Australia, 6th to 13th December 1962-1964, pp.213-241.
- Vogel, S (2013) Comparative Biomechanics: Life's Physical World. Princeton University Press: Princeton, NJ. 90-135, 265-8.
- Webb, PW (1971) The swimming energetics of trout: I. Thrust and power output at cruising speeds. J Exp Biol, 55: 489–520.
- Webb, PW (1975) Hydrodynamics and Energetics of Fish Populations. Bulletin of Fisheries Research Board of Canada, 190: 9-133.
- Webb, PW and Weihs, D (ed.) (1983) Fish Biomechanics. Praeger Publishers: NYC, NY. 59-68, 86-92, 140-67, 181-83, 195-209.
- Wilson, RP (2011) Animal behaviour: The price tag. Nature, 469: 164-165.

- Wilson, RP, Sala, JE, Gómez-Laich, Ciancio, J and Quintana, F (2015) Pushed to the limit: food abundance determines tag-induced harm in penguins. *Animal Welfare*, 24: 37-44.
- Winter, JD (1983) Underwater biotelemetry. In Nielsen, LA and Johnsen, JD eds. *Fisheries Techniques*. 371-395 pp. American Fisheries Society; Bethesda, Maryland.
- Winter, JD (1996) Advances in Underwater biotelemetry. In Murphy, BR and Willis, DW eds., *Fisheries Techniques*, 2nd edition. 555-590 pp. American Fisheries Society; Bethesda, Maryland.

APPENDIX

Table A1: Comparison of trout model measurements and morphological measurements of body parameters collected from museum specimens of lake trout ('lean' variety) as well as the head width-to-total length and peduncle width-to total length ratios.

Sp #	Total Length (cm)	Head Width ¹ (mm)	Peduncle Width ² (mm)	Head width/ total length (mm)	Peduncle width/ total length (mm)
Model	40.0	37.77	11.79	0.0944	0.0295
1	40	36.5	9.62	0.0913	0.0241
2	40.5	41.58	11.05	0.1027	0.0273
3	33.5	32.57	9.75	0.0972	0.0291
4	20.5	19.05	5.41	0.0930	0.0264
5	47	49.19	13.57	0.1047	0.0289
6	53.5	60.29	15.53	0.1127	0.0290
7	50	52.27	15.38	0.1045	0.0308
8	59	59.43	18.26	0.1007	0.0309
9	57.5	66.23	17.98	0.1152	0.0313

Notes:

¹Measured at opercula

²Measured at start of caudal fin

Calculation A1: Calculating blockage corrections for the trout model on a sting in the water tunnel.

$$\text{Blockage ratio} = \frac{\text{Total area of model and sting (cm}^2\text{)}}{\text{Total area of water tunnel test section (cm}^2\text{)}}$$

$$\text{Total area of the model and sting (cm}^2\text{)} = A_{\text{model}} + A_{\text{sting}} + A_{\text{attachment}}$$

$$\text{Total area of the model and sting (cm}^2\text{)} = 37.7 + 125 + 24$$

$$\text{Total area of the model and sting (cm}^2\text{)} = 186.7$$

$$\text{Blockage ratio} = \frac{186.7 \text{ cm}^2}{4904.4 \text{ cm}^2}$$

$$\text{Blockage ratio} = 0.0381 \text{ or } 3.81\%$$

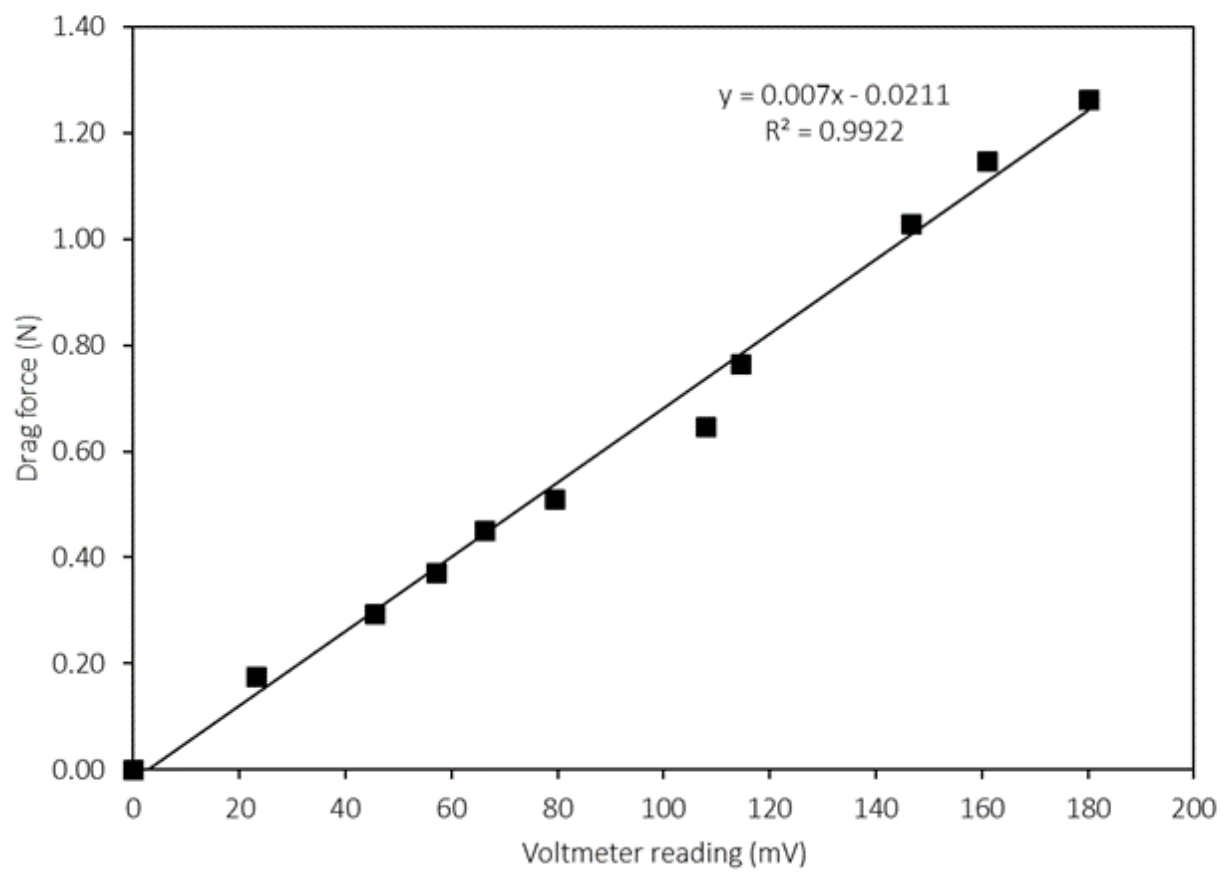


Figure A1: Calibration plot demonstrating linear relationship between voltmeter reading and calculated drag force. The slope of the equation for the line of best fit was used to convert millivolt readings into Newtons.

Table A2: Average velocity (V) (m/s), standard error (V SE) (m/s), tag drag (D) (N), and standard tag drag error (F SE) (N) for all tags (A-F) in chapter 2.

	V (m/s)	V SE (m/s)	D (N)	D SE (N)
Tag A	0.174	0.003	-0.002	0.001
	0.199	0.003	0.003	0.005
	0.225	0.002	0.000	0.005
	0.249	0.003	0.004	0.006
	0.274	0.003	0.005	0.012
	0.301	0.001	0.011	0.013
	0.322	0.003	0.012	0.016
	0.347	0.002	0.000	0.008
	0.362	0.000	0.001	0.006
Tag B	0.174	0.003	0.005	0.001
	0.197	0.003	0.008	0.005
	0.223	0.002	0.000	0.005
	0.249	0.002	0.004	0.006
	0.273	0.002	0.005	0.010
	0.298	0.002	0.007	0.013
	0.325	0.003	0.013	0.016
	0.349	0.002	0.001	0.008
	0.359	0.003	0.003	0.007
Tag C	0.175	0.003	0.006	0.001
	0.200	0.002	0.009	0.005
	0.225	0.002	0.002	0.005
	0.250	0.002	0.010	0.007
	0.273	0.004	0.011	0.011
	0.299	0.002	0.013	0.013
	0.323	0.004	0.019	0.016
	0.346	0.002	0.008	0.008
	0.359	0.001	0.010	0.007
Tag D	0.175	0.003	-0.004	0.001
	0.201	0.003	0.009	0.006
	0.225	0.002	0.007	0.005
	0.251	0.002	0.010	0.006
	0.274	0.002	0.011	0.011
	0.300	0.002	0.011	0.014
	0.321	0.002	0.013	0.017
	0.348	0.002	0.009	0.008
	0.361	0.001	0.003	0.007
Tag E	0.174	0.003	0.003	0.004
	0.198	0.004	0.003	0.005
	0.223	0.002	0.000	0.005
	0.247	0.002	0.004	0.006
	0.273	0.002	0.010	0.010

	0.297	0.005	0.009	0.013
	0.323	0.002	0.013	0.016
	0.345	0.002	0.006	0.011
	0.360	0.001	0.009	0.006
Tag F	0.177	0.006	0.002	0.005
	0.198	0.003	0.006	0.005
	0.223	0.004	0.006	0.010
	0.248	0.002	0.009	0.008
	0.272	0.003	0.010	0.011
	0.299	0.001	0.011	0.013
	0.324	0.002	0.016	0.016
	0.345	0.006	0.007	0.009
	0.360	0.001	0.005	0.008

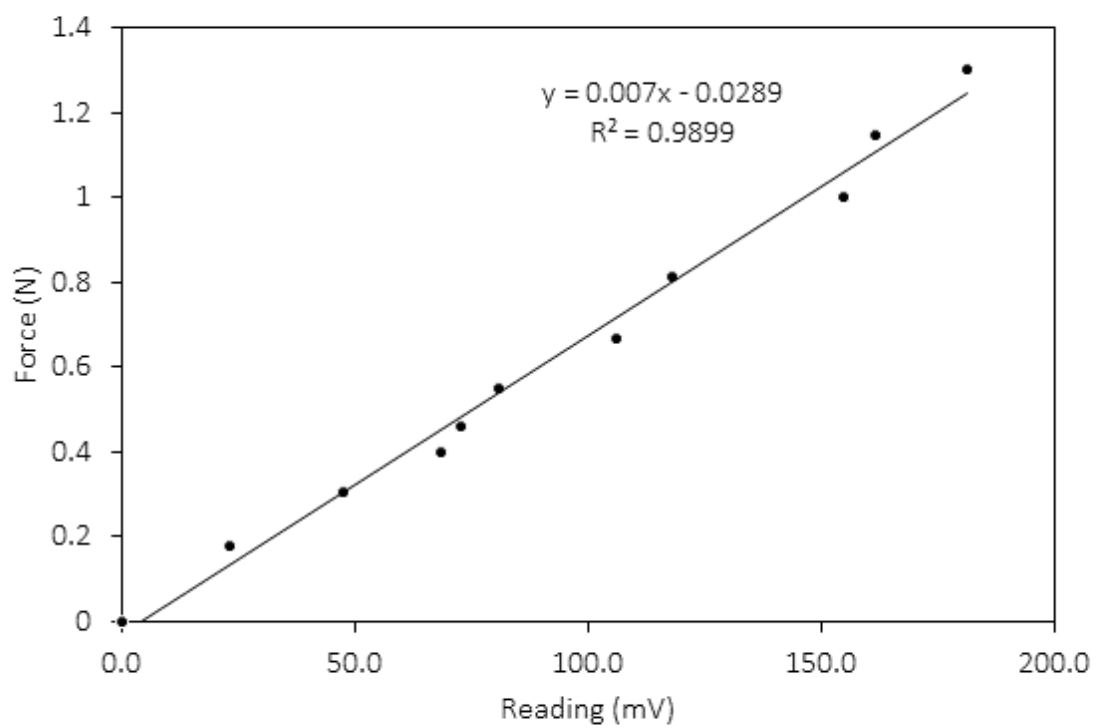


Figure A2: Calibration plot demonstrating linear relationship between voltmeter reading and calculated drag force. The slope of the equation for the line of best fit was used to convert millivolt readings into Newtons.

Table A3: Average water velocity (V) (m/s), standard error of water velocity (V SE) (m/s), average tag drag (D) (N) and standard error of tag drag (D SE) (N) for tag A in chapter 3 at each of the four attachment locations on the fish.

	75%				85%				100%			
	V (m/s)	V SE (m/s)	D (N)	D SE (N)	V (m/s)	V SE (m/s)	D (N)	D SE (N)	V (m/s)	V SE (m/s)	D (N)	D SE (N)
Location 1	0.178	0.004	-0.004	0.008	0.178	0.004	0.002	0.008	0.177	0.004	0.004	0.008
	0.198	0.003	0.009	0.006	0.198	0.003	0.006	0.006	0.195	0.006	0.004	0.006
	0.226	0.002	0.008	0.007	0.224	0.002	0.009	0.007	0.220	0.002	0.010	0.007
	0.248	0.005	0.006	0.006	0.246	0.005	0.010	0.006	0.246	0.002	0.005	0.006
	0.271	0.004	0.005	0.005	0.269	0.004	0.013	0.005	0.276	0.004	0.010	0.005
	0.292	0.004	0.007	0.004	0.300	0.003	0.015	0.004	0.298	0.003	0.013	0.004
	0.320	0.004	0.009	0.003	0.320	0.004	0.027	0.003	0.320	0.004	0.013	0.003
	0.344	0.004	0.006	0.001	0.341	0.004	0.021	0.001	0.345	0.004	0.023	0.002
	0.356	0.002	0.011	0.005	0.353	0.004	0.026	0.005	0.357	0.003	0.018	0.005
Location 2	0.177	0.004	0.004	0.008	0.176	0.004	0.004	0.008	0.177	0.004	0.010	0.008
	0.198	0.002	0.002	0.006	0.196	0.002	0.008	0.006	0.198	0.002	0.008	0.006
	0.220	0.002	0.005	0.007	0.226	0.002	0.002	0.007	0.222	0.002	0.012	0.007
	0.249	0.001	0.010	0.006	0.251	0.003	0.012	0.006	0.246	0.001	0.012	0.006
	0.274	0.004	0.017	0.005	0.272	0.004	0.013	0.005	0.270	0.004	0.012	0.005
	0.298	0.003	0.009	0.004	0.297	0.005	0.012	0.005	0.295	0.004	0.012	0.004
	0.317	0.004	0.017	0.003	0.316	0.004	0.017	0.003	0.314	0.004	0.024	0.004
	0.347	0.004	0.019	0.001	0.340	0.005	0.021	0.001	0.340	0.004	0.021	0.001
	0.359	0.003	0.015	0.006	0.356	0.004	0.028	0.005	0.358	0.003	0.034	0.005
Location 3	0.170	0.004	0.000	0.008	0.175	0.004	0.005	0.008	0.178	0.004	0.006	0.008
	0.197	0.004	0.002	0.006	0.194	0.002	0.005	0.006	0.197	0.002	0.010	0.006
	0.222	0.007	0.000	0.007	0.222	0.003	0.000	0.007	0.220	0.002	0.007	0.007
	0.246	0.004	0.004	0.006	0.247	0.003	0.013	0.006	0.248	0.002	0.017	0.006
	0.268	0.006	0.012	0.005	0.273	0.005	0.011	0.005	0.274	0.005	0.017	0.005
	0.300	0.004	0.010	0.004	0.297	0.004	0.012	0.004	0.296	0.004	0.022	0.004
	0.319	0.004	0.016	0.003	0.323	0.005	0.017	0.003	0.321	0.007	0.020	0.004
	0.345	0.004	0.016	0.001	0.350	0.004	0.018	0.001	0.342	0.004	0.016	0.001
	0.358	0.005	0.023	0.005	0.361	0.003	0.015	0.006	0.357	0.002	0.013	0.005

Location 4	0.175	0.004	-0.003	0.008	0.168	0.005	-0.001	0.008	0.174	0.005	0.004	0.008
	0.200	0.002	-0.006	0.006	0.198	0.003	0.007	0.006	0.194	0.003	0.002	0.006
	0.224	0.003	0.002	0.007	0.228	0.002	0.008	0.007	0.223	0.002	0.009	0.007
	0.246	0.002	-0.001	0.006	0.250	0.002	0.006	0.006	0.246	0.003	0.007	0.007
	0.272	0.006	0.007	0.005	0.271	0.004	0.013	0.005	0.267	0.005	0.022	0.005
	0.300	0.003	0.014	0.004	0.297	0.004	0.005	0.004	0.296	0.004	0.018	0.005
	0.322	0.004	0.010	0.004	0.320	0.004	0.020	0.003	0.324	0.004	0.024	0.003
	0.348	0.004	0.012	0.001	0.342	0.004	0.019	0.001	0.345	0.004	0.012	0.001
	0.356	0.002	0.010	0.005	0.355	0.002	0.018	0.005	0.359	0.003	0.013	0.005

Table A4: Average water velocity (V) (m/s), standard error of water velocity (V SE) (m/s), average tag drag (D) (N) and standard error of tag drag (D SE) (N) for tag B in chapter 3 at each of the four attachment locations on the fish.

	75%				85%				100%			
	V (m/s)	V SE (m/s)	D (N)	D SE (N)	V (m/s)	V SE (m/s)	D (N)	D SE (N)	V (m/s)	V SE (m/s)	D (N)	D SE (N)
Location 1	0.175	0.004	-0.001	0.008	0.173	0.004	-0.004	0.020	0.175	0.004	0.003	0.008
	0.197	0.002	0.001	0.006	0.197	0.004	-0.004	0.027	0.196	0.002	0.003	0.006
	0.224	0.002	-0.002	0.007	0.222	0.002	-0.004	0.027	0.223	0.005	-0.001	0.007
	0.251	0.003	-0.003	0.006	0.249	0.002	-0.005	0.027	0.248	0.002	0.008	0.006
	0.273	0.004	0.003	0.005	0.273	0.004	-0.003	0.033	0.273	0.004	0.008	0.005
	0.300	0.003	0.001	0.005	0.299	0.003	-0.002	0.038	0.296	0.003	0.006	0.004
	0.322	0.004	0.008	0.004	0.324	0.004	0.003	0.027	0.321	0.004	0.016	0.003
	0.346	0.004	0.002	0.001	0.347	0.005	0.002	0.026	0.346	0.006	0.012	0.001
	0.358	0.002	0.006	0.006	0.360	0.003	0.006	0.005	0.359	0.002	0.021	0.005
Location 2	0.175	0.004	0.002	0.008	0.174	0.005	-0.005	0.008	0.148	0.035	0.002	0.008
	0.200	0.004	0.003	0.006	0.197	0.003	-0.002	0.006	0.197	0.002	0.001	0.006
	0.225	0.002	-0.003	0.007	0.223	0.003	-0.010	0.007	0.223	0.002	0.000	0.007
	0.249	0.002	0.000	0.006	0.247	0.002	-0.008	0.006	0.247	0.003	0.001	0.006
	0.274	0.004	0.011	0.005	0.274	0.005	0.000	0.006	0.271	0.005	0.007	0.006
	0.297	0.003	0.002	0.005	0.297	0.003	0.002	0.005	0.295	0.006	0.006	0.004
	0.325	0.005	0.008	0.005	0.320	0.004	0.008	0.004	0.321	0.004	0.013	0.003
	0.351	0.004	0.010	0.001	0.348	0.005	0.003	0.001	0.342	0.005	0.013	0.001
	0.361	0.003	0.008	0.006	0.360	0.002	0.009	0.005	0.359	0.003	0.016	0.008
Location 3	0.173	0.004	-0.001	0.008	0.172	0.004	-0.001	0.008	0.172	0.004	0.003	0.008
	0.197	0.002	0.002	0.006	0.198	0.002	0.002	0.006	0.198	0.003	0.006	0.006
	0.222	0.002	-0.004	0.007	0.221	0.002	-0.002	0.007	0.226	0.002	0.009	0.007
	0.247	0.001	0.001	0.006	0.248	0.001	-0.001	0.006	0.248	0.001	0.006	0.006
	0.271	0.004	0.010	0.005	0.275	0.004	0.003	0.005	0.272	0.004	0.006	0.005
	0.298	0.003	0.003	0.005	0.295	0.004	0.003	0.005	0.296	0.004	0.009	0.005
	0.320	0.004	0.003	0.003	0.321	0.004	0.008	0.004	0.320	0.004	0.015	0.004
	0.347	0.004	0.006	0.003	0.346	0.004	0.008	0.001	0.340	0.004	0.016	0.002
	0.358	0.003	0.012	0.007	0.358	0.002	0.013	0.005	0.357	0.004	0.016	0.006

Location 4	0.174	0.004	-0.004	0.008	0.170	0.005	0.001	0.008	0.178	0.004	0.002	0.008
	0.197	0.004	-0.003	0.006	0.197	0.005	0.006	0.006	0.197	0.005	0.004	0.006
	0.222	0.002	-0.006	0.007	0.223	0.002	0.001	0.007	0.223	0.005	-0.007	0.007
	0.248	0.002	-0.004	0.006	0.251	0.003	0.004	0.006	0.251	0.002	-0.002	0.006
	0.273	0.004	0.002	0.005	0.273	0.005	0.009	0.005	0.273	0.004	0.002	0.007
	0.300	0.003	-0.004	0.006	0.320	0.003	0.014	0.032	0.301	0.003	0.004	0.004
	0.320	0.004	0.002	0.006	0.339	0.004	0.018	0.005	0.321	0.004	0.009	0.003
	0.345	0.006	0.006	0.002	0.361	0.004	0.015	0.001	0.350	0.006	0.007	0.002
	0.355	0.003	0.004	0.007					0.357	0.002	0.006	0.005

Table A5: Average water velocity (V) (m/s), standard error of water velocity (V SE) (m/s), average tag drag (D) (N) and standard error of tag drag (D SE) (N) for tag C in chapter 3 at each of the four attachment locations on the fish.

	75%				85%				100%			
	V (m/s)	V SE (m/s)	D (N)	D SE (N)	V (m/s)	V SE (m/s)	D (N)	D SE (N)	V (m/s)	V SE (m/s)	D (N)	D SE (N)
Location 1	0.176	0.005	0.002	0.008	0.180	0.004	0.003	0.008	0.180	0.004	0.003	0.008
	0.197	0.007	0.001	0.006	0.198	0.004	0.003	0.006	0.201	0.004	0.003	0.006
	0.226	0.003	-0.004	0.007	0.224	0.003	0.001	0.007	0.219	0.002	0.003	0.007
	0.251	0.003	0.001	0.006	0.244	0.003	0.010	0.006	0.248	0.001	0.000	0.006
	0.273	0.006	0.006	0.006	0.269	0.004	0.012	0.005	0.273	0.004	0.005	0.005
	0.298	0.008	0.008	0.004	0.299	0.003	0.017	0.004	0.302	0.004	0.006	0.004
	0.325	0.004	0.009	0.003	0.322	0.005	0.013	0.003	0.324	0.007	0.015	0.004
	0.345	0.005	0.003	0.001	0.343	0.007	0.009	0.001	0.340	0.007	0.017	0.002
0.357	0.002	0.004	0.005	0.358	0.005	0.014	0.005	0.360	0.002	0.018	0.006	
Location 2	0.178	0.004	0.003	0.008	0.177	0.005	0.001	0.008	0.175	0.004	-0.002	0.008
	0.201	0.002	0.002	0.006	0.198	0.004	0.005	0.006	0.198	0.004	0.006	0.006
	0.220	0.004	-0.002	0.007	0.221	0.009	-0.002	0.007	0.221	0.002	-0.004	0.007
	0.246	0.002	0.003	0.006	0.245	0.004	0.004	0.006	0.247	0.004	0.002	0.006
	0.275	0.006	0.003	0.005	0.272	0.005	0.021	0.005	0.272	0.005	0.009	0.005
	0.294	0.003	-0.002	0.004	0.299	0.004	0.014	0.004	0.295	0.003	0.002	0.004
	0.319	0.004	0.015	0.003	0.324	0.004	0.017	0.003	0.319	0.004	0.014	0.003
	0.341	0.004	0.011	0.001	0.344	0.004	0.011	0.002	0.347	0.004	0.017	0.001
0.358	0.002	0.012	0.005	0.355	0.002	0.019	0.005	0.357	0.003	0.019	0.005	
Location 3	0.178	0.005	-0.002	0.009	0.173	0.005	0.002	0.008	0.172	0.005	0.001	0.008
	0.196	0.006	0.003	0.006	0.200	0.003	0.002	0.006	0.198	0.003	0.001	0.006
	0.222	0.003	-0.004	0.007	0.222	0.004	-0.002	0.007	0.226	0.002	-0.001	0.007
	0.251	0.002	-0.001	0.006	0.248	0.002	0.002	0.006	0.248	0.003	0.002	0.006
	0.274	0.005	0.008	0.006	0.274	0.005	0.003	0.005	0.272	0.005	0.008	0.005
	0.299	0.007	0.009	0.005	0.299	0.003	0.006	0.004	0.296	0.003	0.000	0.004
	0.322	0.010	0.015	0.004	0.323	0.006	0.011	0.003	0.320	0.005	0.005	0.004
	0.346	0.007	0.009	0.003	0.343	0.005	0.010	0.001	0.340	0.004	0.010	0.001
0.355	0.002	0.014	0.005	0.357	0.004	0.016	0.005	0.357	0.002	0.013	0.006	

Location 4	0.176	0.004	0.003	0.008	0.172	0.006	0.000	0.008	0.174	0.004	0.000	0.008
	0.199	0.003	-0.002	0.006	0.198	0.002	0.004	0.006	0.200	0.002	0.001	0.006
	0.223	0.006	-0.011	0.008	0.224	0.002	0.003	0.007	0.224	0.004	0.003	0.007
	0.250	0.002	-0.005	0.006	0.246	0.006	-0.001	0.006	0.246	0.003	0.003	0.006
	0.275	0.005	0.006	0.005	0.273	0.007	0.008	0.006	0.279	0.004	0.015	0.005
	0.297	0.003	0.008	0.004	0.295	0.005	0.011	0.004	0.296	0.006	0.006	0.006
	0.319	0.004	0.011	0.003	0.322	0.004	0.008	0.003	0.323	0.004	0.016	0.004
	0.348	0.005	0.009	0.001	0.350	0.004	0.005	0.001	0.343	0.004	0.007	0.001
	0.358	0.002	0.006	0.005	0.357	0.003	0.009	0.005	0.360	0.003	0.018	0.006
